Journal of Soils and Sediments (2022) 22:3189–3208
https://doi.org/10.1007/s11368-022-03326-5

SEDIMENTS, SEC 2 • PHYSICAL AND BIOGEOCHEMICAL PROCESSES • RESEARCH ARTICLE

Factors controlling ^{137}Cs distribution in bottom sediments of Koronowo Reservoir (Poland)

Ilona Sekudewicz[1] · Šárka Matoušková[2] · Zuzanna Ciesielska[3] · Anna Mulczyk[1] · Michał Gąsiorowski[1]

Received: 23 May 2022 / Accepted: 23 August 2022 / Published online: 3 September 2022

Abstract

Purpose The main aim of this study was to investigate factors influencing the long-term distribution of ^{137}Cs activity concentrations in the bottom sediments of the dam lake, Koronowo Reservoir, 32 years after the Chernobyl nuclear power plant accident. For this purpose, selected properties of the collected sediment samples, such as grain size, mineralogical composition, and organic matter (OM) content, were investigated.

Materials and methods The samples of lake sediments were collected with a Kayak-type gravity corer. The spatial and vertical distributions of ^{137}Cs and ^{40}K activity concentrations in the bottom sediments were investigated based on gamma spectrometry measurements. The particle size distribution of surface lake sediments was determined using a laser particle size analyzer. SEM and XRD were used for the mineralogical analysis of the collected sediment samples. Additionally, the content of organic matter was examined in all samples using an elemental analyzer.

Results The ^{137}Cs content was significantly elevated in the case of fine-grained (< 63 μm) surface lake sediments (classified as silts, which are deposited in the profundal zone of Koronowo Lake) and ranged from 12.5 ± 4.1 to 29.2 ± 4.0 Bq kg^{-1}. It was found that the increased concentration of ^{137}Cs activity is more closely related to the content of the silt fraction (2–63 μm) than to the clay fraction (< 2 μm) in the collected surface lake sediments. The content of clay minerals also showed a significant positive correlation with ^{137}Cs activity concentration in the surface lake sediments of Koronowo Lake. A similar relationship was noticed for the OM content, but it may be suspected that it is the result of radiocesium-bearing particle accumulation in OM-rich sediments.

Conclusion The most important factor influencing the spatial distribution of ^{137}Cs activity concentrations in the surface lake sediments of Koronowo Lake, apart from the bottom morphology and grain size of sediments, is the content of clay minerals. Moreover, the increased detrital inflow to the lake after the construction of the dam could have probably affected the vertical distribution of ^{137}Cs activity concentrations in the bottom sediments, as evidenced by, e.g., the measurements of ^{40}K activity concentration.

Keywords Cesium-137 · Potassium-40 · Lake sediments · Chernobyl fallout · Mineralogical composition · Grain-size distribution

Responsible editor: Olivier Evrard

✉ Ilona Sekudewicz
i.sekudewicz@twarda.pan.pl

[1] Institute of Geological Sciences, Polish Academy of Sciences, ul. Twarda 51/55, 00-818 Warszawa, Poland

[2] Institute of Geology, Czech Academy of Sciences, Rozvojová 269, 165 00 Prague, Czech Republic

[3] Institute of Geological Sciences, Polish Academy of Sciences, ul. Senacka 1, 30-063 Kraków, Poland

1 Introduction

Radiocesium ^{137}Cs has been released into the environment as a result of nuclear weapon tests and nuclear power plant accidents, e.g., in Chernobyl and Fukushima (e.g., Ashraf et al. 2014; Beresford et al. 2016; Evrard et al. 2020). Due to its high affinity for fine particles, this isotope is immobilized readily in soils and sediments (He and Walling 1996; Zachara et al. 2002; Park et al. 2021). As a result, ^{137}Cs can be used as a time marker for sediment dating or as an indicator of soil erosion (e.g., Appleby 2008; Zapata and Nguyen

2009; Putyrskaya et al. 2020). The deposited ^{137}Cs has also been redistributed within and beyond contaminated areas by surface process such as fluvial transport (e.g., Tanaka et al. 2015; Ivanov et al. 2021). Diaz-Asencio et al. (2017) emphasized that intensified erosion of a catchment area increases the load of particles and thus the influx of pollutants into the fluvial system. Moreover, anthropogenic changes in river morphology (related to, e.g., dam construction) may affect the storage of sediments contaminated with ^{137}Cs (Kurikami et al. 2014; Díaz-Asencio et al. 2017; Funaki et al. 2019; Sekudewicz and Gąsiorowski 2022). As a consequence, the reservoirs may trap significant amounts of radiocesium-bearing particles, which can also pose a serious environmental risk if this radionuclide is rereleased into the fluvial system (Ivanov et al. 2021). On the other hand, bottom sediments can provide a valuable source of information concerning the long-term redistribution of ^{137}Cs (Konoplev et al. 2019). On this basis, changes in, e.g., the level of contamination of transported particles by ^{137}Cs or the sediment load can be reconstructed.

The distribution of ^{137}Cs in lake sediments is significantly related to the characteristics of the lake and its catchment area, and sediment properties such as particle size, mineralogical composition and organic matter (OM) content (He and Walling 1996; Fan et al. 2014; Tanaka et al. 2015; Tachi et al. 2020a, b; Park et al. 2021; etc.). One of the most important factors that may affect the accumulation and distribution of ^{137}Cs in freshwater ecosystems are transport processes and related sorting of sediment particles (e.g., Tanaka et al. 2015; Huon et al. 2018). It has been widely observed that the concentration of ^{137}Cs activity generally increases while the particle size decreases (He and Walling 1996; Fan et al. 2014; and others). This increase is because the fine-sized (< 63 μm) particle fraction is characterized, e.g., by a large specific surface area and an increased content of clay minerals, which affects the binding of ^{137}Cs and makes it an important carrier of this radionuclide (He and Walling 1996; Spezzano 2005; Funaki et al. 2019; Mouri 2020). Therefore, studying the particle transport processes and the properties of sediments may be the key to understanding the behavior of radiocesium in freshwater ecosystems (Fan et al. 2014). However, it should also be noted that the relation between the distribution of radiocesium and the grain size of sediment particles still remains unclear (Hagiwara et al. 2020). It was observed, for example, that the silt-size (2–63 μm) particle fraction of bottom sediments at the midstream Kuchibuto, Kuroiwa, and Fushiguro sites contains more ^{137}Cs than the clay-size (< 2 μm) particle fraction (Tanaka et al. 2015).

Another important factor that could influence the accumulation of ^{137}Cs in lake sediments is their mineralogical composition (Ashraf et al. 2014; Tanaka et al. 2015; Huon et al. 2018; Hagiwara et al. 2020). This influence is due to the sorption and fixation of Cs is particularly determined by the type and amount of phyllosilicate minerals (Sawhney 1972; Zachara et al. 2002; Tachi et al. 2020a; Park et al. 2021). Depending on their different physicochemical properties, such as chemical composition, expandability, cation exchange capacity (CEC), and layer charge, they are able to bind Cs to varying degrees (Cornell 1993; Mukai et al. 2016; Park et al. 2021). Moreover, in the case of clay minerals, the sorption of Cs is highly controlled by the specific sorption at frayed edge sites (FES) and the exchangeable sorption at regular exchange sites (RES) (Sawhney 1972; Cornell 1993; Zachara et al. 2002; Tachi et al. 2020b). The mineralogical composition of lake sediments can be additionally used to trace the origin of particles contaminated with ^{137}Cs (Hagiwara et al. 2020). It may indicate, for example, whether the accumulated particles originate from eroded surrounding rocks or were produced within the reservoir (Díaz-Asencio et al. 2017). It was also found that ^{40}K can be used as an indicator of detrital layers in sediment records (Putyrskaya et al. 2020). The validity of the use of ^{40}K in the study of sediment distribution was also emphasized by Somboon et al. (2018), who indicated that such analyses can readily help to reveal differences in the mineral composition of sediment samples.

Understanding the role of OM in the distribution of ^{137}Cs is also very important, as it can affect the mobility and bioavailability of radiocesium in freshwater ecosystems (Kaminski et al. 1994; Staunton et al. 2002; Fujii et al. 2018). On the other hand, the adsorption of radiocesium by OM is rather negligible; therefore, the mechanism of ^{137}Cs accumulation in OM-enriched sediments still remains unclear (Fujii et al. 2018). Moreover, it is known that the presence of OM might even inhibit the sorption of Cs^+ on clay minerals by blocking access to FESs (Rigol et al. 2002; Fan et al. 2014; Suga et al. 2014). Therefore, the accumulation of ^{137}Cs can be more closely related to a combination of factors determining its immobilization, such as the grain size of sediment particles, their mineral composition, and OM content (Kim et al. 2007; Fujii et al. 2018; Tachi et al. 2020b). In addition, the composition of OM can be used as an indicator of anthropogenic impacts or environmental changes (Meyers and Ishiwatari 1993; Contreras et al. 2018). For instance, it may indicate the origin of organic particles, as it is known that the C/N ratio for nonvascular aquatic plants is typically between 4 and 10, while for vascular terrestrial plants, it is greater than 20 (Prahl et al. 1980; Ertel and Hedges 1984; Meyers and Ishiwatari 1995; Lamb et al. 2006; Contreras et al. 2018). On this basis, the C/N ratio is considered to be a representative proxy of the origin of OM deposited in freshwater sediments.

The main aim of the present study was to investigate the major factors influencing the distribution of ^{137}Cs activity concentrations in the bottom sediments of Koronowo Lake 32 years after the Chernobyl nuclear power plant accident. For this purpose, the most critical factors that can

potentially affect the migration and accumulation of ^{137}Cs in lake sediments (grain size, mineralogical composition, and OM content) were investigated. To better track the transport processes occurring in Koronowo Lake, the origin of organic particles in the collected lake sediments was determined based on C/N ratio measurements. For the same purposes, the mineralogical composition of inorganic particles and the concentration of ^{40}K activity in the collected sediment samples were analyzed. Selected parameters of the collected sediment cores were also examined to investigate factors influencing the vertical distribution of ^{137}Cs activity concentrations in the bottom sediments of Koronowo Lake. The obtained data were used to reconstruct changes in sedimentation processes and to assess their potential impact on the delivery and redistribution of radiocesium-bearing particles in this reservoir over time.

2 Materials and methods

2.1 Study area

The study area was located in the main basin of Koronowo Lake (Fig. 1). This lake is an artificial reservoir that was created in 1961. It is situated in the lower part of the Brda River (left tributary of the Vistula River) in the lowland in northern Poland. The surface area, capacity volume level, maximum, and mean water depth of Koronowo Lake are 1560 ha, 81.0 million m^3, 21.2 m, and 5.7 m, respectively. The catchment area of the studied lake is equal to 4299 km^2 and is mainly covered with agricultural lands and forests (Szatten et al. 2018). The average discharge of the Brda River (the main tributary of Koronowo Lake) in 1962–2015 was approximately 23.7 m^3 s^{-1} (Hydropower Plant Koronowo 2015). The sediment budget in this lake is dominated by suspended sediments, which are delivered mainly by the Brda River. The total load of sediments supplied from the upper basin of the Brda River to Koronowo Lake in 2015 was estimated to be 2439 t, while their outflow from the lake was approx. 1743 t (Szatten et al. 2018).

The main basin of Koronowo Lake is located from Wielonek to the dam in Pieczyska (Fig. 1A). It contains 32.7 million m^3 of water, which constitutes over 1/3 of all water retained in this reservoir. It is the main area for sediment accumulation, especially in the zones near the dam, estuary of inflows, and bays (Szatten et al. 2018). This part of the lake is also characterized by more limnetic conditions with increased biological production in the bays. The main basin of this lake is located in an area formed mainly by glacial outwash sands and gravels (Fig. 1B). In the northern part, there are also humic sands and silts, while in the southern part (near the dam), glacial tills and deluvial sands occur. The northern part of the study area is

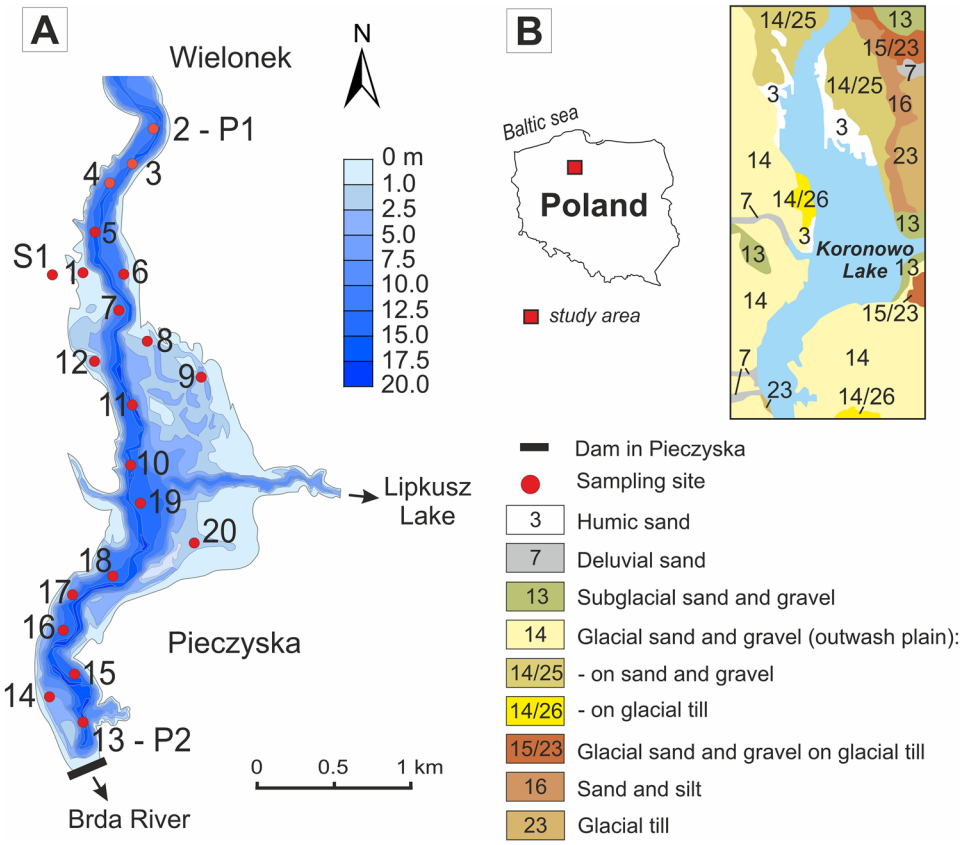

Fig. 1 Sampling area **A** (Szatten 2016; modified) and geological setting **B** of Koronowo Lake (Wieczorek and Stoiński 2008; modified)

located mainly in an uncultivated area covered with coniferous forest, while in the southern part, there are more buildings, marinas, and recreational areas.

2.2 Sampling and sample treatment

A fieldwork campaign was carried out on the main basin of Koronowo Lake in October 2018 (Fig. 1). One soil profile, 20 surface lake sediment samples, and 2 sediment cores were collected. The soil profile (S1) had a length of 25-cm depth and was divided in the field into 4 sections depending on the lithology (Fig. S1; Supplementary Material). Lake sediments were collected using a Kayak-type gravity corer (55 mm in internal diameter). Surface lake sediments (0–3-cm depth) were collected in 6 transects from the littoral and profundal zones of the lake. Sediment cores were taken from the deepest points of the lake's bottom in the northern part of the main basin (core P1: sampling site 2, lake depth: 9 m, profile length: 32 cm) and in the southern part near the dam (core P2: sampling site 13, lake depth: 15 m, profile length: 27 cm). The sediment cores were divided in the field into 1-cm thick slices. All samples were packed in plastic bags and stored in a refrigerator at 4 °C. Then, all samples were transported to the laboratory, where they were weighed, dried (for 48 h at 60 °C), homogenized, and prepared for the analyses.

2.3 Grain-size and elemental analysis

The grain size distribution of surface lake sediments was measured using sieve analysis (for particles > 1000 µm) and a CILAS 1190 laser particle size analyzer at the Institute of Geology CAS. The instrument was set in wet dispersion mode, providing a range from 0.04 to 1000 µm. The data were obtained after dispersion in KOH, removing carbonates by HCl and removing organic matter by H_2O_2 and HNO_3. The obtained results are reported in three fractions: clay (up to 2 µm), silt (2–63 µm), and sand (63–2000 µm). Surface sediments were classified according to the Shepard sediment classification diagram (Shepard 1954) using the "ggtern" R package (Hamilton and Ferry 2018).

The contents of total organic carbon (TOC) and total nitrogen (TN) were measured in all collected samples using a Vario CUBE elemental analyzer. Sulfanilic acid was used as a standard for analysis. Prior to analysis, carbonates were removed from the samples with 5% hydrochloric acid. Milled and homogenized samples (5–6 mg) were transferred into tin capsules. The uncertainties of the TOC and TN measurements were lower than 0.6% and 0.18%, respectively.

2.4 XRD and SEM–EDS analyses

All surface lake sediment samples and selected samples from sediment cores P1 (at 20-cm depth) and P2 (at 6-cm and 27-cm depth) were examined using X-ray and SEM–EDS methods. Mixtures of powdered samples, the internal standard (10 wt.% ZnO), and 4 ml of methanol were milled in a McCrone micronizing mill for 5 min to obtain homogenous samples with narrow grain-size distributions. Then, the specimens were prepared for X-ray analysis using the side-loading method, which minimizes the preferred orientation (Środoń et al. 2001). The mineral composition of the samples was determined with a Thermo Electron ARL X'TRA diffractometer at Clay Minerals Laboratory in the Institute of Geological Sciences PAS. It is equipped with a 12-position sample holder and a Peltier cooled solid-state detector operating in a Bragg–Brentano geometry using CuKα radiation (40 kV, 30 mA). Diffraction patterns were collected in a 2θ range of 2.5–65° with a step size of 0.02° (5 s/step).

Qualitative and quantitative analyses were performed using Q-min software, which works based on a combination of the mineral intensity factor (MIF) technique and preregistered pure standards collection. Determination of mineral composition was achieved by fitting the measured XRD pattern of the sample with patterns of pure standards (Środoń et al. 2001). During matching, some ranges were excluded from matching, and some were optimized with higher weights. These were the ranges with stable reflections of the internal standard and clay minerals.

The accuracy of the quantitative XRD analysis depends to a large extent on the crystallinity of the selected phases—the higher the crystallinity is, the higher the sensitivity and precision of this method. For example, in the case of phases such as calcite, gypsum, anhydrite, and ankerite/dolomite, their detection is possible in the presence of even below approximately 1%, while for smectitic clay minerals, it is approximately 5%. The precision of the obtained results also depends on the crystallinity of the phases, but generally, it can be assumed to be equal to ± 3–5% of the absolute values (Raven and Self 2017).

The surface lake sediment samples were analyzed using a scanning electron microscope (SEM) FE-SIGMA VP (Carl Zeiss Microscopy GmbH) in conjunction with two energy-dispersive X-ray spectrometers (Quantax XFlash 6|10, Bruker Nano GmbH). The powdered samples were placed on an aluminum mount with conductive carbon tape and coated with a carbon layer (20 nm) with a vacuum coater (Quorum 150 T ES). Analyses were performed with a 60-µm aperture and 20-keV acceleration voltage.

2.5 Gamma spectroscopy

The concentrations of ^{137}Cs and ^{40}K activity in all collected samples were measured using a low background gamma spectrometer (Canberra-Packard) with a Broad Energy Germanium (BE5030) detector (FWHM = 1.28 keV at 661.7 keV for ^{137}Cs and 1.72 keV at 1460.8 keV for ^{40}K). All samples were analyzed in a round polyethylene cup (flat cylinder geometry). The energy calibration was performed using a radioactive standard. The reference material IAEA-SL-2 was used to verify the quality of the measurements. The obtained spectra were analyzed with Genie 2000 software. The average counting time per sample ranged from 24 to 72 h. The counting time and uncertainty of the measurements depended on the minimal detection activity (MDA) and the sample mass (from 2 to 45 g). The uncertainty of the ^{137}Cs and ^{40}K activity concentration measurements ranged from 11 to 39% and from 9 to 44%, respectively. The MDA of ^{137}Cs and ^{40}K varied from 0.34 to 6.8 Bq kg^{-1} and from 4.4 to 81.3 Bq kg^{-1}, respectively. All measured ^{137}Cs and ^{40}K activity concentrations were converted to the first day of sampling (October 24, 2018).

2.6 Data analysis

^{137}Cs, ^{40}K, and TOC and TN spatial distribution maps were generated using the inverse distance weighting (IDW) interpolation method ArcGIS ver. 10.6 (Esri Co., Ltd., Redlands, CA, USA). Statistical analyses were performed using R 4.0.3 (R Core Team 2020). The Shapiro−Wilk test (confidence level 95%) was used to test the normal distribution of the analyzed data. Spearman's rank correlation coefficients were calculated to assess the relationship (p value < 0.05) between measured variables. To conduct a principal component analysis (PCA), the data were centered, scaled, and then tested to examine their suitability using the Kaiser−Meyer−Olkin (KMO) test.

3 Results

3.1 Surface lake sediments

3.1.1 Particle size distribution and organic matter content

The surface lake sediments were classified as fine- (< 63 µm) and coarse-grained (> 63 µm) sediments. According to Shepard's classification diagram, the fine-grained sediments were classified as silt (sample nos. 2–5, 7, 10, 11, 13, 15, 16, and 18–19), whereas the coarse-grained sediments were recognized as sand (sample nos. 6, 8, 9, 14, 17, and 20) and silty sand (sample nos. 1 and 12) (Figs. 2 and 3). The obtained data showed that the grain size of surface lake sediments is

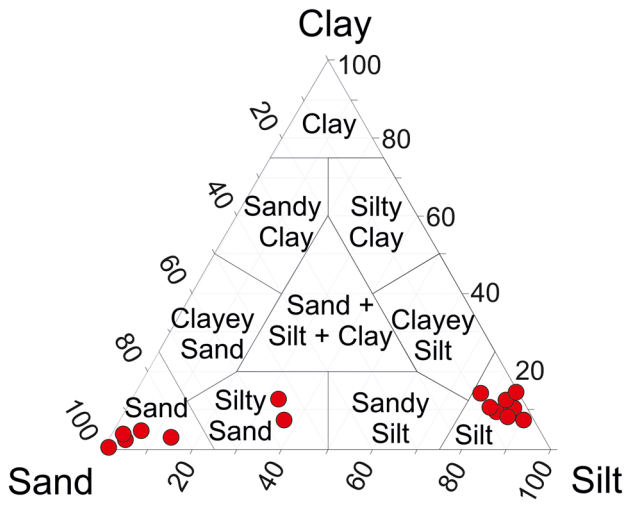

Fig. 2 Shepard's classification diagram of surface (0–3-cm depth) lake sediments in Koronowo Lake

significantly related to the depth of the reservoir (Table 1). Most fine-grained surface lake sediments occur in the "old," pre-reservoir Brda Valley, where the lake is now the deepest (Fig. 1). The sand fraction dominates ($R_s = -0.61$, p value < 0.05) in the littoral zone, whereas the clay ($R_s = 0.49$, p value < 0.05) and silt fractions ($R_s = 0.62$, p value < 0.05) dominate in the profundal zone of the lake (Table 1). The silt fraction prevails in all fine-grained surface lake sediments (Fig. 3A). A relatively high content of clay fraction was also observed in samples collected from the shallower (at approx. 2 m of a depth) part of the lake (sampling sites no. 12 (12.4%) and 1 (8.6%)). The average water content of fine- (arithmetic mean, $n = 12$) and coarse-grained bottom sediments (arithmetic mean, $n = 8$) was 89% and 31%, respectively, whereas the average wet bulk density was 1.08 g cm^{-3} and 1.63 g cm^{-3}, respectively.

The average contents of TOC and TN in fine-grained surface lake sediments (arithmetic mean, $n = 12$) were 17.9% and 2.6%, respectively, while those in coarse-grained surface lake sediments (arithmetic mean, $n = 8$) were 1.3% and 0.3%, respectively. The elevated content of OM (expressed as the content of TOC and TN) was observed mainly in the case of fine-grained bottom sediments deposited in the deepest parts of Koronowo Lake (Figs. 4 and 5). The content of OM in surface lake sediments deposited in the littoral zone was much lower than that in the profundal zone, except for sands collected at sampling sites no. 1 and 17 (in which the content of TOC was up to 3.4% and 5.2%, respectively). The C/N ratio calculated for fine-grained surface lake sediments ranged from 5.4 to 9.3. Due to the results being below the detection limit, it was not possible to calculate the C/N ratio for coarse-grained surface lake sediments, except for samples no. 1 (C/N = 20.9), 14 (C/N = 4.5), and 17 (C/N = 5.5).

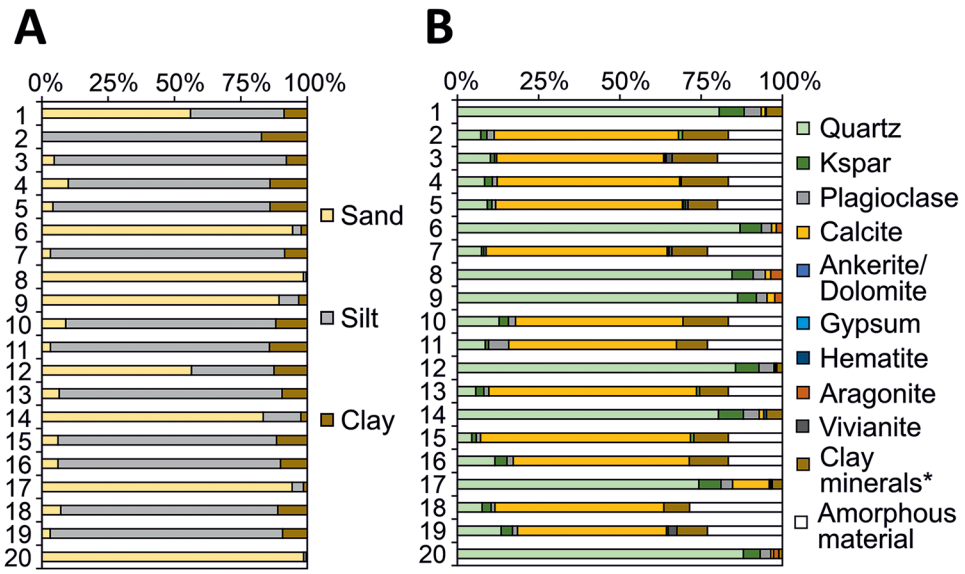

Fig. 3 Grain-size distribution **A** and mineralogical composition **B** of surface (0–3-cm depth) lake sediments in Koronowo Lake. Sampling sites are presented in Fig. 1

3.1.2 XRD and SEM-SEM analyses

Silts were mainly composed of calcite (up to ~ 65%), amorphous material (up to ~ 30%), clay minerals (muscovite, chlorite, kaolinite, smectite group, and illite−smectite) (from ~ 8 to ~ 14%), quartz (up to ~ 13%), and an admixture of plagioclase, potassium feldspar, gypsum, ankerite/dolomite, and vivianite (Fig. 3B). The sands and silty sands were mainly composed of quartz (up to ~ 88%), calcite (up to ~ 11%), potassium feldspar (up to ~ 8%), clay minerals (up to ~ 5%), plagioclase (up to ~ 5%), and an admixture of aragonite, gypsum, ankerite/dolomite, and hematite. The highest contents of the kaolinite, muscovite, illite−smectite, and smectite group in silts were approximately 1.6, 3.8, 7.4, and 9.6%, respectively. In the case of sands and silty sands, the muscovite and smectite group were not identified, while the highest concentrations of kaolinite, chlorite, and illite−smectite were approximately 1.3, 0.4, and 4.9%, respectively. The most enriched fine-grained bottom sediments in clay minerals were samples no. 2, 3, and 10. In the case of coarse-grained bottom sediments, the highest content of clay minerals was observed in samples no. 1, 14, and 17. The contents of clay minerals, amorphous material, and calcite in the surface lake sediments of Koronowo Lake are significantly positively correlated with the depth of the lake, the silt and clay fraction contents, and ^{137}Cs and OM contents (Table 1). They are also significantly negatively correlated with the wet bulk density of the collected bottom sediments and the contents of ^{40}K, sand fraction, quartz, potassium feldspar, and plagioclase.

The SEM−EDS analyses showed that the amorphous material was represented mainly by the remains of organic debris composed of amorphous silica and organic material (Fig. 6A–C). Based on the conducted analyses, the presence of quartz, calcite, potassium feldspar, plagioclase, and clay minerals was confirmed. The presence of authigenic calcite (Fig. 7A) and vivianite (Fig. 7C) was observed in the case of fine-grained surface lake sediments. Additionally, iron oxyhydroxides (Fig. 6D) and framboidal pyrites (Fig. 7D) were also recognized. The presence of monazite, zircon, hematite, and titanium oxides (e.g., samples no. 14, 17) was observed in the case of sands and silty sands (Fig. 7B).

3.1.3 Spatial distribution of ^{137}Cs and ^{40}K activity concentrations

The ^{137}Cs content in the surface lake sediments of Koronowo Lake is characterized by a bimodal distribution, which is related to the elevated content of this radionuclide in fine-grained sediments and the decreased content in coarse-grained bottom sediments (Figs. 4 and 5). The average ^{137}Cs activity concentrations in fine-grained bottom sediments are almost four times higher (17.67 ± 3.96 Bq kg^{-1}; arithmetic mean, $n = 12$) than in coarse-grained bottom sediments (5.08 ± 0.82 Bq kg^{-1}; arithmetic mean, $n = 8$). Relatively high concentrations of ^{137}Cs activity were also measured in sample no. 14 (21.2 ± 2.6 Bq kg^{-1}) and 17 (7.8 ± 1.3 Bq kg^{-1}), which contain significant amounts of sandy fraction (Fig. 3A).

Similar to ^{137}Cs, the content of ^{40}K in the surface lake sediments of Koronowo Lake is also characterized by a bimodal distribution. In the case of fine-grained bottom sediments, the content of ^{40}K is lower (160.2 ± 36.7 Bq kg^{-1}; arithmetic mean, $n = 12$) than in coarse-grained bottom sediments (237.9 ± 22.0 Bq kg^{-1}; arithmetic mean, $n = 8$). The highest concentrations of ^{40}K activity were detected in the surface lake sediments collected from sampling site no. 1

Table 1 Spearman's rank correlation among the measured parameters in surface (0–3-cm depth) lake sediments of Koronowo Lake. Correlation coefficients > 0.4 and with p value ≤ 0.05 are bolded

	^{137}Cs	^{40}K	TN	TOC	Wt	Blk	Depth	Sand	Clay	Silt	Qtz	Kfs	Pg	Cal	Ill-Smc	Smc	Am	Cl
^{137}Cs	**1.00**																	
^{40}K	**−0.46**	**1.00**																
TN	**0.76**	**−0.73**	**1.00**															
TOC	**0.60**	**−0.70**	**0.85**	**1.00**														
Wt	**0.67**	**−0.71**	**0.85**	**0.89**	**1.00**													
Blk	**−0.64**	**0.67**	**−0.84**	**−0.93**	**−0.97**	**1.00**												
Depth	**0.60**	**−0.75**	**0.78**	**0.75**	**0.74**	**−0.73**	**1.00**											
Sand	**−0.55**	**0.54**	**−0.65**	**−0.65**	**−0.65**	**0.71**	**−0.61**	**1.00**										
Clay	0.24	−0.36	**0.48**	**0.66**	**0.66**	**−0.72**	**0.49**	**−0.66**	**1.00**									
Silt	**0.66**	**−0.60**	**0.68**	**0.66**	**0.65**	**−0.69**	**0.62**	**−0.93**	**0.50**	**1.00**								
Qtz	**−0.50**	**0.69**	**−0.74**	**−0.88**	**−0.83**	**0.88**	**−0.77**	**0.75**	**−0.62**	**−0.75**	**1.00**							
Kfs	−0.37	**0.79**	**−0.64**	**−0.71**	**−0.66**	**0.65**	**−0.66**	**0.75**	**−0.51**	**−0.71**	**0.77**	**1.00**						
Pg	−0.43	**0.75**	**−0.59**	**−0.51**	−0.44	0.40	**−0.61**	**0.51**	−0.19	**−0.61**	**0.60**	**0.68**	**1.00**					
Cal	**0.47**	**−0.77**	**0.72**	**0.84**	**0.83**	**−0.84**	**0.73**	**−0.69**	**0.59**	**0.66**	**−0.92**	**−0.78**	**−0.68**	**1.00**				
Ill-smc	**0.58**	−0.28	**0.64**	**0.56**	0.41	**−0.46**	**0.55**	**−0.67**	0.37	**0.60**	**−0.53**	**−0.49**	**−0.46**	0.38	**1.00**			
Smc	**0.51**	**−0.54**	**0.57**	**0.73**	**0.78**	**−0.79**	**0.52**	**−0.61**	**0.68**	**0.62**	**−0.75**	**−0.68**	**−0.45**	**0.77**	0.26	**1.00**		
Am	**0.62**	**−0.67**	**0.79**	**0.70**	**0.69**	**−0.68**	**0.68**	**−0.83**	**0.54**	**0.80**	**−0.69**	**−0.81**	**−0.64**	**0.63**	**0.69**	**0.55**	**1.00**	
Cl	**0.57**	**−0.45**	**0.61**	**0.71**	**0.65**	**−0.70**	**0.59**	**−0.80**	**0.66**	**0.74**	**−0.76**	**−0.76**	**−0.54**	**0.69**	**0.71**	**0.81**	**0.72**	**1.00**

^{137}Cs activity concentration (Bq kg^{-1}), ^{40}K activity concentration (Bg kg^{-1}), *TN* total nitrogen (%), *TOC* total organic carbon (%), *Wt.* water content (%), *Blk.* wet bulk density (g cm^{-3}), *Depth* depth of the lake at sampling point (m), *Sand* sand fraction (%), *Clay* clay fraction (%), *Silt* silt fraction (%), *Qtz* quartz (%), *Kfs* potassium feldspar (%), *Pg* plagioclase (%), *Cal* calcium (%), *Ill-Smc* illite–smectite (%); *Smc* smectite group (%), *Am.* amorphous material (%), *Cl.* sum of clay minerals (kaolinite, muscovite, chlorite, illite–smectite, smectite group) (%)

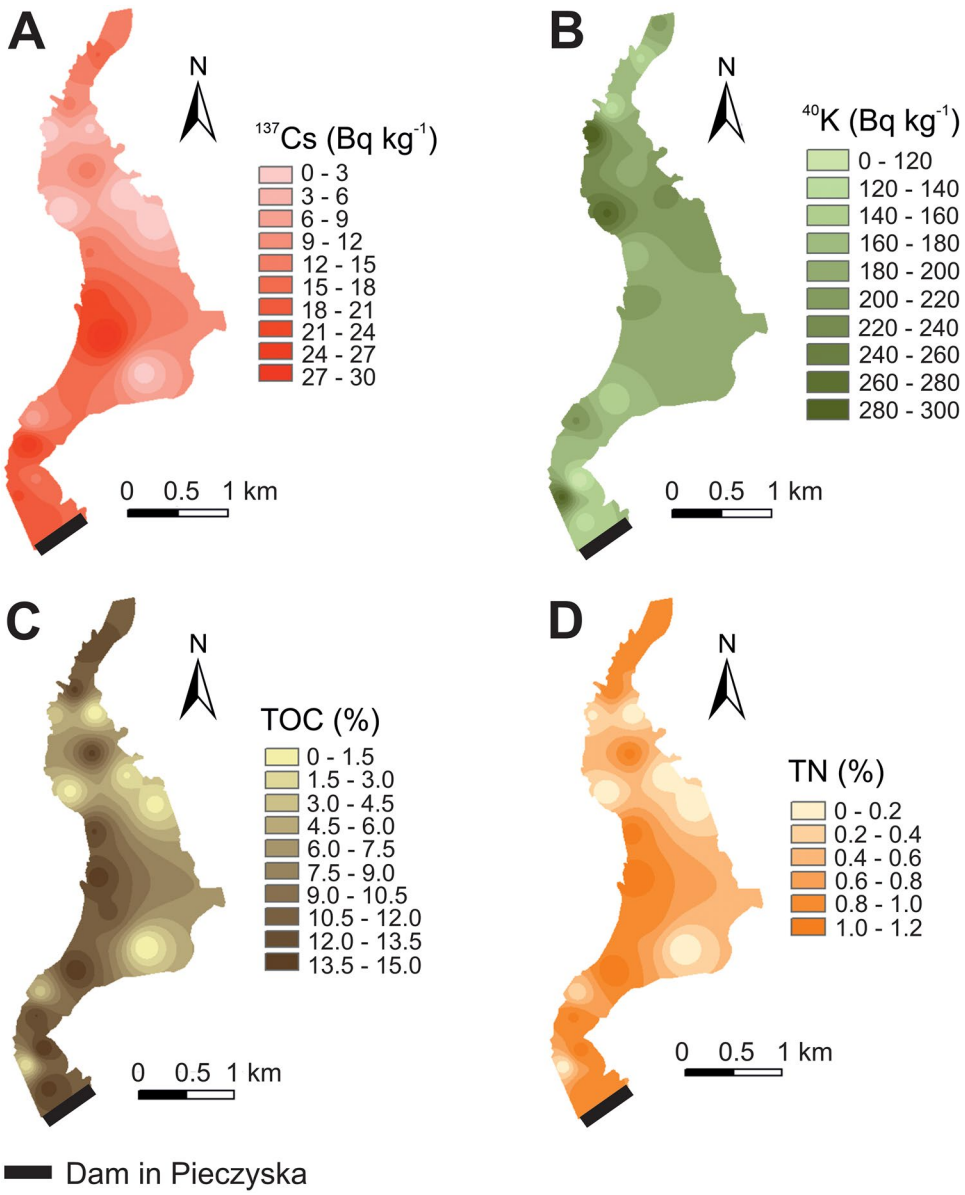

Fig. 4 Spatial distribution of **A** ^{137}Cs and **B** ^{40}K activity concentrations (Bq kg^{-1}), **C** total organic carbon (TOC), and **D** total nitrogen (TN) (%) content in surface (0–3-cm depth) lake sediments of Koronowo Lake

(299.1 ± 26.3 Bq kg^{-1}), 12 (282.1 ± 25.5 Bq kg^{-1}), and 14 (284.48 ± 24.85 Bq kg^{-1}).

The spatial distributions of ^{137}Cs and ^{40}K activity concentrations in the surface lake sediments of Koronowo Lake are presented in Fig. 4. They showed that bottom sediments deposited in the profundal zone of the lake contain more ^{137}Cs than in the littoral zone, which is the opposite in the case of ^{40}K. Apart from the depth of the lake, the ^{137}Cs content is also significantly positively correlated with the silt fraction, amorphous material, clay minerals (especially illite−smectite and smectite group), and organic matter (expressed as TOC and TN) in the surface lake sediments of Koronowo Lake (Table 1; Fig. 8). There is also a significant negative correlation between ^{137}Cs and the sand fraction, quartz content, and wet bulk density of the collected sediment samples. The content of ^{40}K is significantly positively correlated with the wet bulk density of the collected sediment samples and the contents of sand fraction, quartz, potassium feldspar, and plagioclase. There is also a significant negative correlation between the content of ^{40}K and amorphous material, calcite, clay minerals, and OM in these surface lake sediments.

3.1.4 PCA results

The PCA of selected parameters indicates that Axis 1 and Axis 2 explained 78% and 8.6% of the variance of the components, respectively (Fig. 8). The first PCA axis (PC1) was dominated by high positive loading of the depth of the lake and the content of ^{137}Cs, TOC, clay minerals, silt, and clay fraction and by high negative loading of the wet bulk density and the content

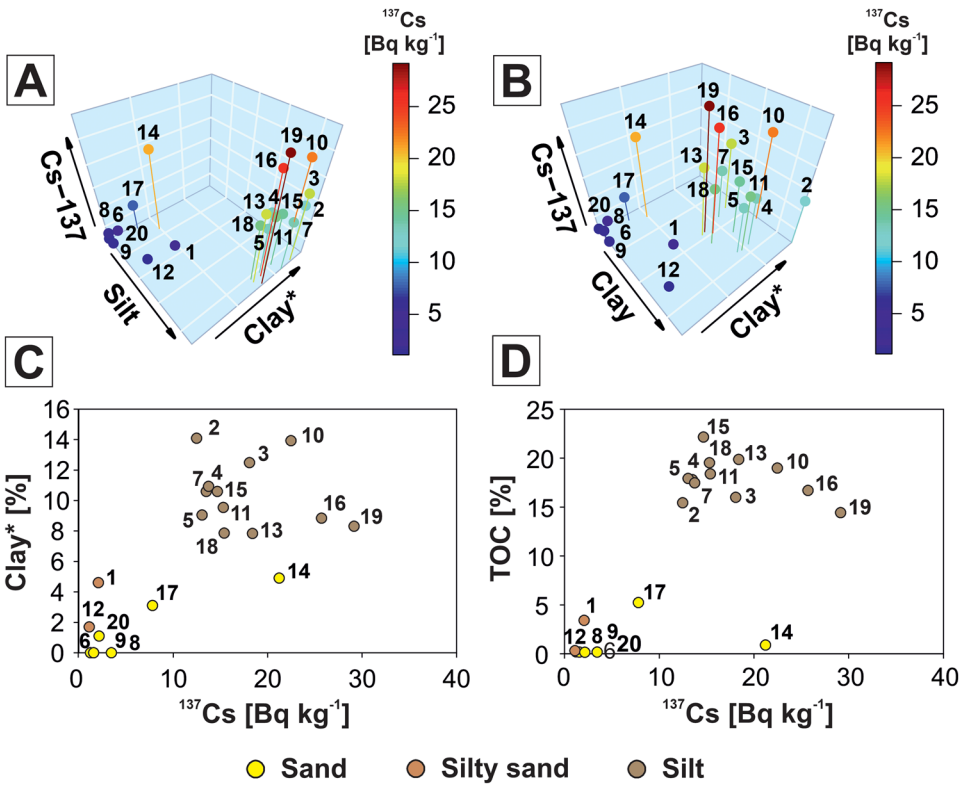

Fig. 5 Correlation on the 3D graph between ^{137}Cs activity concentration (Bq kg^{-1}), **A** Clay*—sum of clay minerals (kaolinite, muscovite, chlorite, illite–smectite, and smectite group (%)), Silt—silt fraction (%), and **B** Clay—clay fraction (%). Correlation on the 2D graph between the content of ^{137}Cs (Bq kg^{-1}), **C** Clay* minerals (%), and **D** total organic carbon (TOC) (%) in surface (0–3-cm depth) lake sediments of Koronowo Lake. Sampling sites are presented in Fig. 1

of potassium feldspar and quartz. ^{137}Cs showed high positive loading to the first (PC1) axis (R^2 = 0.74, p < 0.001). Potassium ^{40}K, instead of ^{137}Cs, had high negative loading to the first (PC1) axis (R^2 = -0.72, p < 0.001) and high positive loading to the second (PC2) axis (R^2 = 0.66, p < 0.001).

The PCA biplot shows that the surface lake sediments of Koronowo Lake can be divided into three groups. The first group includes fine-grained sediments (silts) with significantly elevated contents of ^{137}Cs, clay minerals, and OM. The second group is represented by coarse-grained sediments (sands) characterized by higher values of wet bulk density. These sediments are also characterized by elevated contents of ^{40}K, quartz, and potassium feldspar and low contents of ^{137}Cs. The last group is represented by coarse-grained sediments with a higher silt fraction (samples no. 1, 12, and 14). This group is also characterized by low concentrations of ^{137}Cs activity (except for sample no. 14, which contains 21.2 ± 2.6 Bq kg^{-1} of ^{137}Cs) and elevated concentrations of ^{40}K activity.

3.2 Lake sediment columns

3.2.1 Lithology, mineralogical composition, and organic matter content

The lithology of core P1 (sampling site no. 2) was constant along the entire length of the sediment column and was presented by brown silts up to a depth of 29 cm, where the presence of black sand with organic debris was observed (Fig. 9). Similarly, in core P2 (sampling site no. 13), brown silts were also observed with no significant changes in lithology over the entire length of the sediment column. The average wet bulk densities in core P1 (arithmetic mean, n = 32) and core P2 (arithmetic mean, n = 27) were 1.3 g cm^{-3} and 1.1 g cm^{-3}, respectively. In core P1, the wet bulk density of sediments was variable along the entire length of the sediment column with a slight increase from a depth of 19 cm, while in core P2, it was much more constant with a slight increase from a depth of 25 cm.

The mineralogical composition of lake sediments in the top part (0–3-cm depth) of core P1 was the same as that in the surface sediment sample at sampling site no. 2 (Fig. 3B). At a depth of 20 cm, the mineralogical composition of the collected sediment samples differed significantly from that in the surface layer of the sediment column. A much lower content of calcite (~ 25%) and amorphous material (~ 13%), as well as elevated contents of quartz (~ 18%), potassium feldspar (~ 5%), gypsum (~ 4.3%), and plagioclase (~ 3.4%) with an admixture of anhydrite (~ 0.8%) and ankerite/dolomite (~ 0.7%), were observed. Additionally, a significant increase in the content of clay minerals (from ~ 14 to ~ 30%) was recognized in this sediment layer, where illite−smectite, smectite group, muscovite/phlogopite, and chlorite were equal to approximately 17%, 5.6%, 5%, and 3%, respectively.

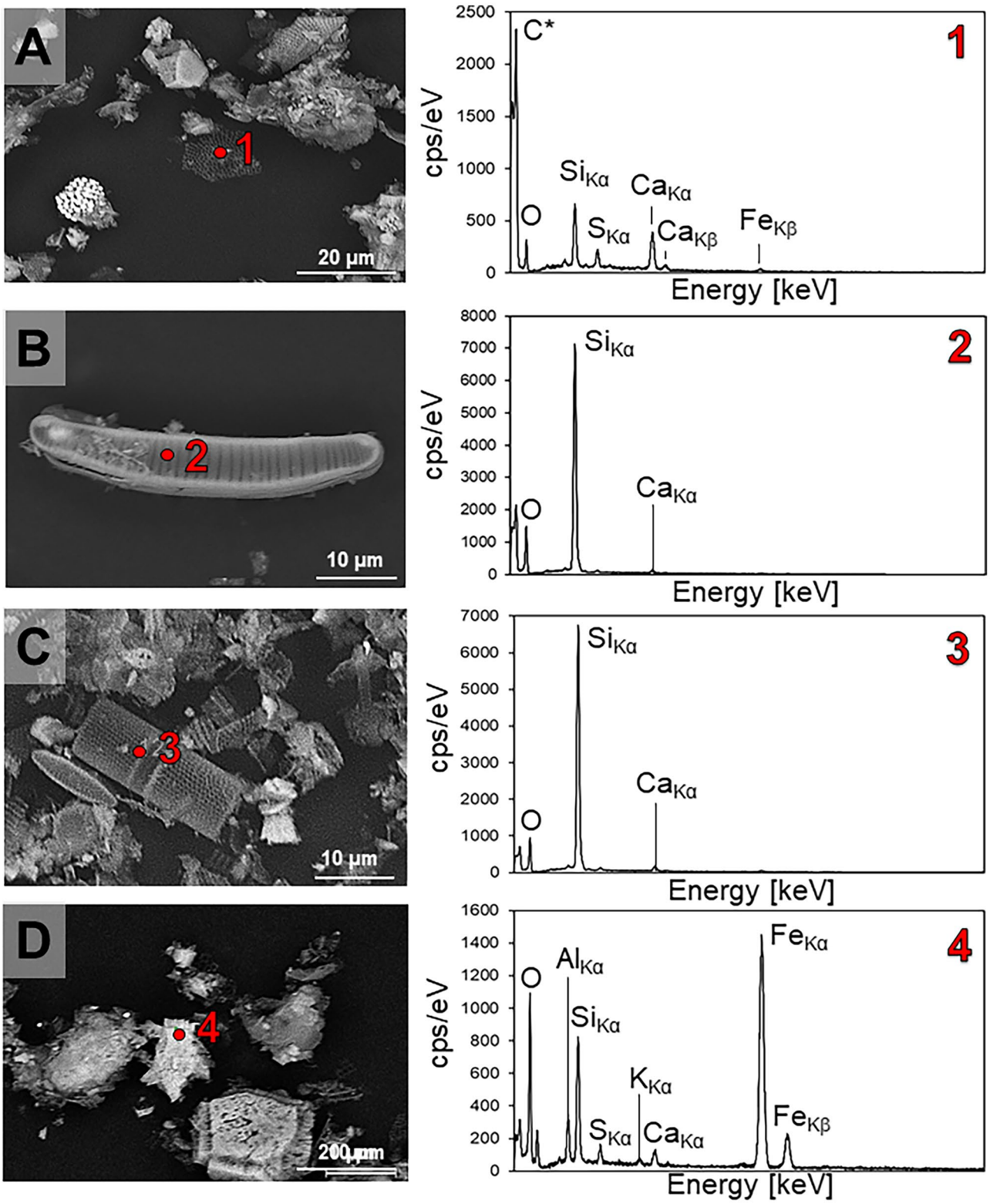

Fig. 6 The SEM–EDS analysis of surface (0–3-cm depth) lake sediments in Koronowo Lake. **A** Organic matter (sample no. 13). **B** Organic debris (diatom *Eunotia* spp.) (sample no. 2). **C** Organic debris (diatom *Aulacoseira* spp.) (sample no. 19). **D** Iron oxyhydroxides (sample no. 3). Sampling sites are presented in Fig. 1

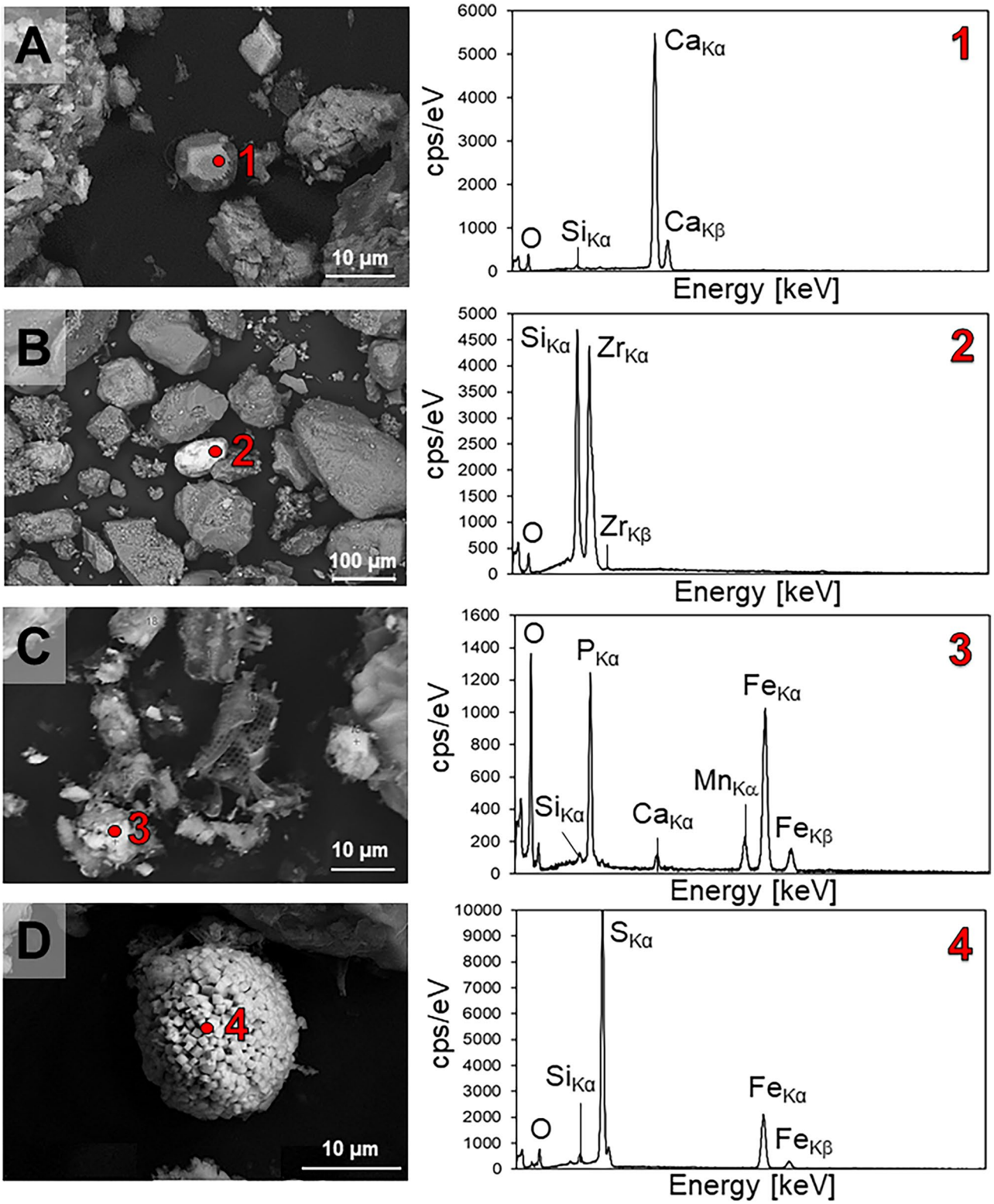

Fig. 7 The SEM–EDS analysis of surface (0–3-cm depth) lake sediments in Koronowo Lake. **A** Authigenic calcite (sample no. 13). **B** Zircon (sample no. 14). **C** Vivianite (sample no. 3). **D** Framboidal pyrite (sample no. 14). Sampling sites are presented in Fig. 1

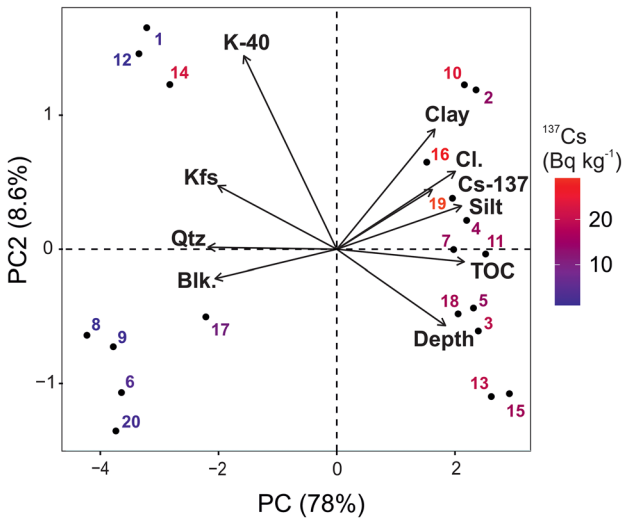

Fig. 8 The PCA biplot based on the selected parameters in surface (0–3-cm depth) lake sediments of Koronowo Lake: *Cs-137*, activity concentration (Bq kg^{-1}); *K-40,* activity concentration (Bg kg^{-1}); *TOC,* total organic carbon (%); *Blk.*, wet bulk density (g cm^{-3}); *Depth*, depth of the lake at sampling point (m); *Clay*, clay fraction (%); *Silt*, silt fraction (%); *Qtz*, quartz (%); *Kfs*, potassium feldspar (%); *Cl.*, sum of clay minerals (kaolinite, muscovite, chlorite, illite–smectite, smectite group) (%). Sampling sites are presented in Fig. 1

The mineralogical composition of lake sediments in the surface layer (0–3-cm depth) of core P2 was the same as that in the surface sediment sample at sampling site no. 13 (Fig. 3B). At a depth of 6 cm in this core, there was not much difference in the mineralogical composition of the collected sediments compared to the surface layer, except for a slightly lower content of potassium feldspar (by 1%), higher content of calcite (by 2%), presence of chlorite (~ 1.3%), and lack of muscovite. In the bottom part (27-cm depth) of core P2, slightly lower contents of calcite (~ 38%) and amorphous material (~ 13%) and higher contents of quartz (~ 16%), potassium feldspar (~ 5%), gypsum (~ 3%), plagioclase (~ 2.7%), and aragonite (~ 2.2%) were observed. A significant increase in the content of clay minerals (from ~ 8 to ~ 20%), including smectite group (~ 8.6%), illite−smectite (~ 8.3%), chlorite (~ 2.4%), and muscovite (~ 0.7%), was also recognized in this sediment layer. The SEM−EDS analysis confirmed the presence of such mineral phases as potassium feldspar, plagioclase, calcium carbonates, and clay minerals in the selected sediment samples in both cores. The amorphous material, similar to the case of surface lake sediments, was identified mostly as organic debris (e.g., diatoms). Some amounts of zircon, titanium oxides, monazite, and framboidal pyrite were also identified in the selected sediment samples in both cores.

The average contents of TOC and TN were equal to 9.5% and 1.05% in core P1 (arithmetic mean; $n=30$) and 16.6% and 2.1% in core P2 (arithmetic mean; $n=27$), respectively. The contents

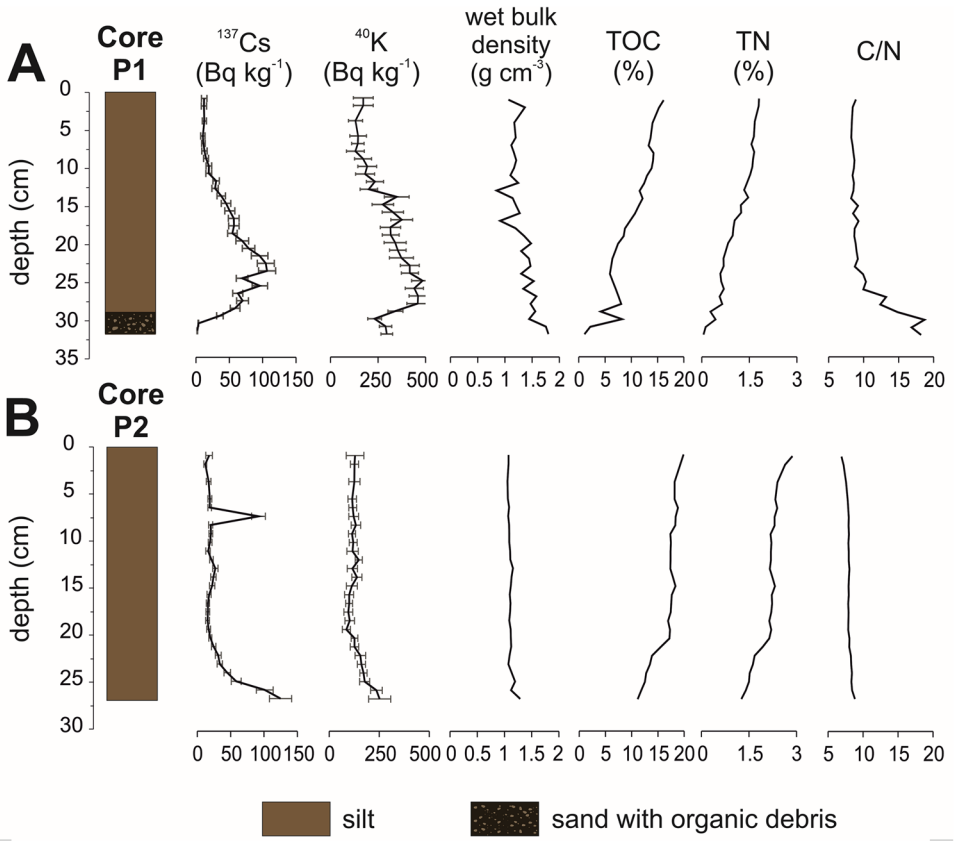

Fig. 9 Lithology and vertical distribution of ^{137}Cs and ^{40}K activity concentrations (Bq kg^{-1}), content of total organic carbon (TOC), and total nitrogen (TN) (%), and C/N ratio in P1 **A** and P2 **B** cores. Sampling sites are presented in Fig. 1

of TOC and TN in core P1 decreased with depth, while core P2 was more constant over the entire length of the sediment column, with a slight decrease from 22 cm depth (Fig. 9). The C/N ratio calculated for lake sediments from the top to a depth of 26 cm of core P1 (C/N ratio ranged from 9.6 to 12.05) indicated the autochthonous origin of deposited OM. At a depth of 30 cm in this core, a significant admixture of terrestrial OM (C/N ratio > 20) was observed (Meyers and Ishiwatari 1993; Lamb et al. 2006; Contreras et al. 2018). The C/N ratio calculated for lake sediments of core P2 also indicated the primary sources of OM (C/N ratio ranged from 8.1 to 10.3) over the entire length of this sediment column.

3.2.2 Vertical distribution of ^{137}Cs and ^{40}K activity concentrations

The vertical distribution of ^{137}Cs and ^{40}K activity concentrations differed significantly between the collected sediment columns (Fig. 9). In core P1 (sampling site. no. 2), an elevated content of ^{137}Cs was observed at depths between 12 and 30 cm in this core. The highest content of ^{137}Cs (106.6 ± 12.8 Bq kg^{-1}) was measured at a depth of 24 cm in this sediment column. A significant decrease in ^{137}Cs content occurred above 30 cm of the core depth, where pre-reservoir sediments were identified. The vertical distribution of ^{137}Cs activity concentrations in core P2 (sampling site no. 13) showed a gradual increase in the content of this radioisotope from a depth of 20 cm (Fig. 9). The highest ^{137}Cs content was observed at the bottom of the core (124.8 ± 16.7 Bq kg^{-1}). A sharp peak in ^{137}Cs content (91.8 ± 10.4 Bq kg^{-1}) was also observed at a depth of 6 cm in this sediment column.

An increase in ^{40}K activity concentration, as in the case of ^{137}Cs, was observed in the sediments located at a depth of approximately 14 to 30 cm in core P1 (Fig. 9). The highest ^{40}K activity concentration (488.2 ± 52.9 Bq kg^{-1}) was measured at a depth of 25 cm in this core. Almost two times lower concentrations of ^{40}K activity were observed in core P2. A gradual increase in the content of ^{40}K was also observed above 20 cm of the core depth. The highest concentration of ^{40}K activity (251.8 ± 55.3 Bq kg^{-1}) was detected, similar to ^{137}Cs, at a depth of 27 cm in this sediment column.

4 Discussion

4.1 Key factors controlling the distribution of ^{137}Cs in bottom sediments of Koronowo Lake

4.1.1 Particle size distribution and transport processes

Grain size is one of the most important factors determining the spatial distribution of ^{137}Cs activity concentrations in the bottom sediments of Koronowo Lake. This is mainly because radiocesium can be easily adsorbed onto fine-sized particles due to their large specific surface area (He and Walling 1996; Fan et al. 2014; Funaki et al. 2019). It is also associated with a higher content of clay minerals (able to bind ^{137}Cs), which are more prevalent in fine-grained sediments (Cremers et al. 1988; Spezzano 2005; Tanaka et al. 2015; Hagiwara et al. 2020). The obtained results showed that fine-grained surface lake sediments of Koronowo Lake contain more ^{137}Cs than coarse-grained surface lake sediments, similar to e.g. the case of the Ogaki Dam Reservoir (Funaki et al. 2019). Moreover, the observed high correlation between the content of ^{137}Cs and silt ($R_s = 0.66$; p value > 0.05) indicated that the silt-sized fraction is a major contributor to the distribution of ^{137}Cs in the studied lake, which was also observed in the case of the Tomioka River (Hagiwara et al. 2020). Tanaka et al. (2015) also noticed that the silt-sized fraction contained a greater amount of ^{137}Cs than the clay-sized fraction, which is supposed to accumulate more radiocesium (Livens and Baxter 1988; Spezzano 2005; Funaki et al. 2019). This phenomenon may be related to the transport of the finest particles by a river in near-permanent suspension (as wash load) and pass through the dam lake without deposition (Tanaka et al. 2015; Sedláček et al. 2022).

The transport processes influencing the sorting of sediment particles may therefore also be responsible for the distribution of ^{137}Cs in the bottom sediments of Koronowo Lake. They may provide, for example, the accumulation of fine-grained particles with ^{137}Cs in the deepest part of the lake (along the course of the river) and near the dam (Figs. 1 and 4A). This is probably caused by the physical transport of smaller radiocesium-bearing particles through the river and its deposition downstream as a result of the decreasing river flow velocity (Carlsson 1978; Spezzano 2005; Tanaka et al. 2015; Hagiwara et al. 2020). The second possible transport mechanism of radiocesium-bearing particles may be horizontal movement, which in a shallow lake (such as Koronowo Lake) may be caused by wind-wave action and river flow (Hilton et al. 1986; Luettich et al. 1990). However, in our case, the horizontal movement might be slightly different than, for example, in a shallow Lake Nishiura (Tsuji et al. 2019). This is because Koronowo Lake is narrower and more elongated, so there may be a gradual movement of sediments with ^{137}Cs from the slopes of the reservoir to the center of the "old Brda valley" and further along the reservoir (Figs. 1 and 4A).

Similar transport processes may also influence the deposition of coarse-grained bottom sediments (characterized by a low content of ^{137}Cs) in the shallower parts of Koronowo Lake (Figs. 1 and 3A). These coarse particles probably originate from the shore of the lake, which is eroded by wind-wave action and/or water-level fluctuations and transported short distances due to their higher settling velocity (Tanaka

et al. 2015; Funaki et al. 2019). Such an origin of these bottom sediments might be evidenced by the presence of allogeneic minerals (such as titanium and zircon), and minerals enriched with potassium ^{40}K (such as potassium feldspar and plagioclase) (Madruga et al. 2014; Hagiwara et al. 2020; Bobos et al. 2021) (Figs. 3B and 7B). This would also explain the heterogeneous spatial distribution of ^{40}K activity concentrations in the surface lake sediments of Koronowo Lake (Fig. 4). In addition, the presence of vascular land plant remains may also indicate the input of terrestrial material into the lake, as indicated by the relatively high C/N ratio (> 20) in these bottom sediments (e.g., at sampling site no. 1) (Meyers and Ishiwatari 1995; Lamb et al. 2006; Contreras et al. 2018).

It should also be noted that in some coarse-grained bottom sediment samples (sampling sites no. 14 and 17), a significantly increased content of ^{137}Cs was observed (Figs. 1 and 5). This indicates that the particle size distribution does not simply explain the spatial distribution of ^{137}Cs activity concentrations in the bottom sediments of Koronowo Lake. Tanaka et al. (2015) also emphasized that the distribution of ^{137}Cs could not be simply related to the specific surface area of the particles due to the complicated origin of riverbed sediments. Somboon et al. (2018) found, for example, that the coarser fractions of material deposited in river channels and floodplain zones might contain significant amounts of radiocesium. In our case, this phenomenon may be hypothetically related to the intensified accumulation of radiocesium-bearing particles near the dam due to a decrease in the flow velocity of the stream and limited outflow from the lake.

4.1.2 Mineralogical composition of surface lake sediments

Apart from the particle size distribution, the mineralogical composition has a very significant influence on the distribution of ^{137}Cs in bottom sediments in aquatic ecosystems (Kim et al. 2006; Fan et al. 2014; Mukai et al. 2016; Hagiwara et al. 2020; and others). Many studies have shown that Cs binding is especially strong with micaceous minerals and their weathered minerals, such as illites and vermiculites (Sawhney 1972; Cremers et al. 1988; Cornell 1993; Poinssot et al. 1999; Park et al. 2021). In our case, clay minerals have a dominant effect on the sorption and thus the distribution of ^{137}Cs in the bottom sediments of Koronowo Lake, which may be evidenced by a significant positive correlation between the content of ^{137}Cs and clay minerals ($R_s = 0.6$, p value < 0.05) (Table 1; Fig. 8). A similar correlation was observed in samples from various regions around the world (Fan et al. 2014; Tanaka et al. 2015; Mukai et al. 2016; Bobos et al. 2021; etc.). However, it should be noted that there are also areas where bottom sediments with similar clay mineral contents are characterized by different ^{137}Cs activity concentrations, e.g., samples collected at sampling sites no. 1 (2.07 ± 0.42 Bg kg^{-1}) and 14 (21.2 ± 2.6 Bq kg^{-1}) (Figs. 1 and 5). This phenomenon may be hypothetically related to a different source and/or level of supplied ^{137}Cs. Regardless, the tendency for an increase in the concentration of ^{137}Cs activity with the amount of clay minerals in the surface lake sediments of Koronowo Lake is maintained.

An increased content of clay minerals was observed, especially in the case of fine-grained surface lake sediments of Koronowo Lake (Fig. 5). A similar relationship was widely reported by many other researchers (Cremers et al. 1988; Tanaka et al. 2015; Funaki et al. 2019; etc.). Moreover, it was noticed that the correlation between the content of clay minerals and silt fraction ($R_s = 0.74$, p value < 0.05) is higher than with the clay fraction ($R_s = 0.66$, p value < 0.05) (Table 1). This relationship may be hypothetically associated with the aggregation of clay minerals (e.g., with organic matter) and their deposition in the reservoir, while other clay size particles are transported downstream (De La Rocha et al. 2008; Tanaka et al. 2015; Fujii et al. 2018).

Among all clay minerals identified in the surface lake sediments of Koronowo Lake, the most abundant were clay minerals 2:1, such as the illite−smectite and smectite group. The relationship between the content of ^{137}Cs and the illite−smectite and smectite group was equal to 0.58 and 0.51 (p value < 0.05), respectively (Table 1). This significant positive correlation can be related to a good sorption capacity of radiocesium by these minerals (Sawhney 1972; Zachara et al. 2002; Kim et al. 2006; Fan et al. 2014; Tachi et al. 2020a; Park et al. 2021). The slight difference in the value of the correlation coefficient between the illite−smectite and smectite group is related to the higher selectivity of Cs^+ by illite (Tamura and Jacobs 1960; Bobos et al. 2021). For other clay minerals, muscovite was identified only in selected samples of fine-grained bottom sediments (sites no. 3, 4, 13, 16, and 19). Although these samples were characterized by increased concentrations of ^{137}Cs activity, no significant correlation was found between the contents of muscovite and ^{137}Cs. Another clay mineral, kaolinite, was identified in small amounts (approximately 1%) and only in several samples. There was also no significant relationship between the content of kaolinite and ^{137}Cs, which may also be explained (apart from its low content) by the fact that 1:1 clay minerals are characterized by low cesium sorption and selectivity (Kim et al. 1996; Park et al. 2021). Other clay minerals, such as chlorite, have been recognized in negligible amounts and therefore do not appear to have a significant effect on ^{137}Cs binding.

Calcium carbonates, such as calcite, were found in significant amounts in fine-grained surface lake sediments characterized by an increased content of ^{137}Cs. This convergence, however, may be accidental and determined by the precipitation of authigenic calcite (Fig. 7A) from the water column in the deep parts of the reservoir, where clay

minerals are dominant (Figs. 1 and 3B). This hypothesis might be supported by Kónya et al. (2005), who showed that calcite practically does not sorb cesium, while dolomite and ankerite show only a slightly greater ability to bind this radionuclide (Kónya et al. 2005). Another calcium carbonate phase, aragonite, was noticed only in coarse-grained surface lake sediments deposited in the coastal zone of the lake. These are likely mollusk shell fragments indicating the probable wave-related bottom erosion in the shallow parts of this reservoir.

Other organic debris (e.g., diatoms) composed of amorphous silica were quite abundant in the bottom sediments collected from the profundal zone of Koronowo Lake (Fig. 6B, C). Despite their high content in the bottom sediments enriched with ^{137}Cs, it is difficult to claim whether their presence influences the fixation of this radioisotope. Belousov et al. (2019) observed that sorption of Cs^+ on diatomite is more related to the presence of kaolinite and smectite in the studied samples. This is probably because the physical adsorption of radiocesium on the mineral surface, which occurs in the case of diatomite, is of less importance than the process of chemical sorption (Nenadović et al. 2015). The second amorphous material, identified in the collected sediment samples by XRD and SEM analyses, is composed of iron oxyhydroxides (Fig. 6A). Their presence may have some significance for ^{137}Cs binding, as it has been found that deposition of $Fe(OH)_3$ on the surface of clay minerals leads to an increase in the sorption of radiocesium (Kobets et al. 2014). Among the iron-containing minerals observed in fine-grained bottom sediments of Koronowo Lake, there were also vivianites and framboidal pyrites (Fig. 7C, D). Their presence does not affect the distribution of ^{137}Cs but indicates the presence of anaerobic conditions in the deep parts of the lake (Wilkin et al. 1996; O'Connell et al. 2015).

A significant negative correlation coefficient ($R_s = -0.50$, p value < 0.05) with the content of ^{137}Cs was demonstrated by quartz, which occurs mainly in coarse-grained surface lake sediments of Koronowo Lake (Table 1). This is because the sorption capacity of radiocesium by quartz is negligibly small (Muuri et al. 2016). The plagioclase and potassium feldspar, also common in the collected sands and silty sands, showed an insignificant negative correlation with this radioisotope (Table 1). This indicates that these minerals have little effect on the distribution of ^{137}Cs activity concentrations in the bottom sediments of Koronowo Lake. However, Hagiwara et al. (2020) have shown that feldspars could contribute to ^{137}Cs migration in the Tomioka River basin. It is also worth noting that the contents of plagioclase ($R_s = 0.75$; p value < 0.05) and potassium feldspar ($R_s = 0.79$; p value < 0.05) in the surface lake sediments of Koronowo Lake show a strong positive correlation with ^{40}K content (Table 1; Fig. 8). This may indicate a possible influx of terrestrial material into the lake, which could have been eroded and transported from the shore by wind-wave actions and/or water-level fluctuations. A similar application of ^{40}K analysis was demonstrated by Bobos et al. (2021), who associated an increased content of this radioisotope with the sediments formed because of granite weathering.

4.1.3 Content of organic matter and its origin

The distribution of radiocesium in soils and sediments may be related to the content of OM; however, the mechanism of ^{137}Cs accumulation in OM-rich sediments is still considered to be unclear (e.g., Naulier et al. 2017; Fujii et al. 2018). In the present study, most organic matter (expressed as the content of TOC and TN) accumulated in fine-grained surface lake sediments deposited in the deepest parts of Koronowo Lake (Figs. 1 and 4). This is probably related to the larger surface area of finer particles, which enable adsorption of the monolayer of organic matter (Keil et al. 1994; Kim et al. 2006). Moreover, such an increase in nutrients and OM from the littoral to the profundal zone was recognized as typical in eutrophic lakes in Poland (Tadejewski 1966; Frink 1969).

Along with an increase in the content of OM in collected bottom sediment samples, an increase in the concentration of ^{137}Cs activity was observed (Fig. 5). This relationship may indicate that OM could play an important role as a carrier of radiocesium in the studied lake, although it has a lower affinity than illite (Rigol et al. 2002; Naulier et al. 2017; Fujii et al. 2018). Kim et al. (2007) observed a similar relationship for marine sediment samples collected from the East Sea near Wuljin, where the TOC content showed an even better correlation with ^{137}Cs activity concentrations than other single factors. Although the PCA in our case can also confirm a high correlation between the content of TOC and ^{137}Cs, the content of clay minerals seems to be of greater importance (Fig. 8). On this basis, we can hypothesize that the observed relationship may result from a combination of various factors, i.e., the accumulation of ^{137}Cs with fine-grained inorganic particles in OM-rich sediments (Kim et al. 2007). Fuji et al. (2018) also explained that this phenomenon can be related to the formation of microaggregates with autochthonous OM and minerals by extracellular polymeric substances. This hypothesis can also be considered in our case, as the examples of microaggregates consisting mainly of clay minerals and OM were observed in the collected sediment samples during SEM analysis. Additionally, the C/N ratio calculated for the collected bottom sediments indicated that OM deposited in the profundal zone of Koronowo Lake is of autochthonous origin (consisting of phytoplankton and to a lesser extent zooplankton), while in the littoral zone, it is rather a mixture of primary production and influx of organic particles washed off from the soil around the lake and fragments of terrestrial plants (Lamb et al. 2006).

It should also be noted that the part of the fine-grained bottom sediments of Koronowo Lake with a significantly elevated content of OM was characterized by average concentrations of ^{137}Cs activity (Fig. 5). Bobos et al. (2021) observed that some OM-rich and fine-grained bottom sediments were characterized by a low ^{137}Cs content. They claimed that this phenomenon may be associated with the inefficient immobilization of radiocesium by clay minerals (e.g., illite) in an environment enriched with OM. A similar mechanism cannot be excluded in our case. Another potential cause of this phenomenon may be the release of ^{137}Cs from lake sediments as a result of ion exchange with, e.g., NH_4^+ (e.g., Evans et al. 1983; Hazotte et al. 2016). Kaminski et al. (1994) noticed that such a process may generally occur in OM-rich sediments of eutrophic lakes, of which Koronowo Lake is an example. Moreover, the presence of minerals (e.g., framboidal pyrite and vivianite) indicating the presence of anaerobic conditions (which may lead to the degradation of OM and the appearance of NH_4^+) may additionally support this assumption. However, to confirm this hypothesis, it may be necessary to examine the chemical composition of the pore water for the presence of competing ions with Cs^+.

4.2 Vertical distribution of ^{137}Cs activity concentrations in bottom sediments of Koronowo Lake

The main source of ^{137}Cs accumulated in the bottom sediments of Koronowo Lake was the Chernobyl accident, but the record of ^{137}Cs deposited as a result of nuclear weapons testing cannot be ruled out, since this reservoir was created in 1961 (Ciesla et al. 1994; Evrard et al. 2020). Moreover, the presented research showed that ^{137}Cs is still supplied to Koronowo Lake despite more than 30 years having passed since the Chernobyl nuclear power plant accident. This is evidenced by the presence of this radioisotope in the surface layer of the collected sediment columns (Fig. 9).

Because the emitted cesium radioisotopes were bound to particles shortly after their direct atmospheric deposition, a distinct peak of ^{137}Cs activity concentration can be commonly observed in the vertical profiles of sediment records in the contaminated areas (Appleby 2008; Klaminder et al. 2012; Beresford et al. 2016; Ivanov et al. 2021; and others). However, this is the case when mixing of sediments is negligible and cesium is strongly bound to the sediments (Konoplev et al. 2022). In our case, the Chernobyl-derived peak in both collected sediment cores is difficult to distinguish and cannot be described, for example, by the Gaussian function, as in the case of the Schekino Reservoir (Ivanov et al. 2021). The vertical distributions of ^{137}Cs activity concentrations in the collected sediment cores may be due to chemical processes, such as advection or diffusion of ^{137}Cs through the pore waters, rather than physical processes, such as sediment mixing by wind-wave action or bioturbation (Robbins et al. 1977; Putyrskaya and Klemt 2007; Klaminder et al. 2012).

The observed shape of the vertical distributions of ^{137}Cs activity concentrations may also be determined by the increased supply of radiocesium to Koronowo Lake along with contaminated particles after the construction of the dam. This hypothesis may be confirmed by the fact that dams significantly affect sedimentation in the river system, converting the reservoirs into major sediment traps (Díaz-Asencio et al. 2017; Funaki et al. 2019). Increased erosion in the catchment area may, in turn, intensify the particle load into the reservoir along with the associated pollutants (Betancourt et al. 2010; Díaz-Asencio et al. 2017). Therefore, the elevated concentrations of ^{137}Cs activity in the sediment profiles could correspond, apart from the direct deposition of radiocesium with atmospheric fallout, to an increased delivery of contaminated particles to Koronowo Lake from its catchment. Subsequently, the amount of supplied ^{137}Cs could have decreased over time as sedimentological conditions stabilized and catchment erosion decreased. This hypothesis can be confirmed by the elevated content of ^{40}K (known as an important indicator of detrital influx) in similar layers of sediment columns as for ^{137}Cs (Somboon et al. 2018; Putyrskaya et al. 2020) (Fig. 9). Similarly, the vertical distribution of the C/N ratio in core P1 showed that the source of OM in these sediment layers was of allochthonous origin and changed over time to primary production. This hypothesis may also be justified by a change in the mineralogical composition of lake sediments in the collected sediment cores, indicating a decrease in the content of deposited quartz and potassium feldspar over time. There is no doubt, however, that additional sediment cores should be collected, and more detailed studies of their mineralogical composition and particle size distribution should be carried out to better support this hypothesis.

The conducted research also showed that the vertical distribution of the analyzed parameters in the collected sediment columns differs significantly from each other (Fig. 9). Although such a small number of collected sediment columns does not allow for the study of changes occurring over time in the entire Koronowo Lake, it is possible to determine the most important differences between the northern and southern parts of this study area. One of them is the higher sedimentation rate in the area near the dam (southern part of the reservoir) than in the northern part of the lake. This undoubtedly influences the observed vertical distribution of ^{137}Cs activity concentration in the collected sediment cores (Fig. 9). A clear boundary is visible between the pre-dam and post-dam sediments in core P1, which makes it possible to calculate the sedimentation rate (0.51 cm y^{-1}) in this part of the lake. Such a boundary has already been associated with reservoir age in other studies and used as an additional time maker to

validate the results of sediment dating with ^{210}Pb or ^{137}Cs (Foster et al. 2011; Waters et al. 2015). No such boundary occurs in core P2, but a significant increase in ^{137}Cs activity concentrations at the bottom of the core can be noticed (Fig. 9). Accordingly, it can be assumed that the Chernobyl-derived peak is probably below a depth of 27 cm in this sediment column. Based on this assumption, it can be concluded that the sedimentation rate in the area near the dam is much higher than that in the northern part of the lake (Fig. 1A). This difference is caused by the preferential particle deposition near the dam due to limited outflow from the reservoir, decreasing river flow, and higher primary production associated with more limnetic conditions in this area (Szatten et al. 2018). Moreover, the sharp increase in the ^{137}Cs content at a depth of 6 cm may be related to mixing of sediments or an accidental influx of contaminated particles from surrounding soils, which are located in a cultivated area. This anomaly may also be related to the increased concentration of ^{137}Cs activity in the coarse-grained surface sediment sample collected at sampling site no. 14 (Figs. 1A and 8). However, to prove this hypothesis, it would be necessary to analyze additional soils and bottom sediment samples from this part of the lake.

5 Conclusions

The obtained results showed that ^{137}Cs is still supplied to the lake, as evidenced by its presence in the collected surface lake sediments. It was observed that the spatial distribution of ^{137}Cs activity concentrations is strongly related to the valley-type bottom morphology of the studied lake. Therefore, the highest content of ^{137}Cs (from 12.5 ± 4.1 to 29.2 ± 4.0 Bq kg^{-1}) was detected in the fine-grained (< 63 μm) bottom sediments collected from the deepest part of the lake, reflecting the "old," pre-reservoir course of the Brda River (in the central part of the lake, where more limnetic conditions prevail and close to the dam). It was also noted that the ^{137}Cs activity concentration was more strongly related to the silt fraction (2–63 μm) than to the clay fraction (< 2 μm) in the collected surface lake sediments.

The conducted research showed that the most important factor influencing the distribution of ^{137}Cs activity concentrations in the surface lake sediments of Koronowo Lake, apart from the bottom morphology and grain size of sediments, is the content of clay minerals. A significant positive correlation was particularly observed between the content of ^{137}Cs and the illite−smectite and smectite group. A positive significant correlation between the content of ^{137}Cs and organic matter (expressed as the content of TOC and TN) was also determined. Moreover, the OM associated with the elevated content of radiocesium was found to be of autochthonous origin. These results may indicate the probable influence of OM on the distribution of ^{137}Cs in the bottom sediments of Koronowo Lake. It can be assumed, however, that this dependence may also be the result of the accumulation of radiocesium-bearing particles in lake sediments rich in OM.

The vertical distribution of ^{137}Cs activity concentrations in the collected sediment cores showed that the Chernobyl-derived peak of radiocesium is not simply represented by a distinct peak associated with direct atmospheric deposition. The observed peak shape may be hypothetically related to the intensified delivery of contaminated sediments with ^{137}Cs from the catchment area as a result of its erosion after the construction of the dam. This hypothesis may be evidenced, for example, by an increased content of ^{40}K at similar depths as ^{137}Cs in the collected sediment columns, which may indicate an intensified detrital influx at that time. This may also be confirmed by the increased content of minerals, such as quartz, plagioclase, and potassium feldspar in the deeper parts of the collected sediment columns. However, to better support this hypothesis, additional cores should be collected, and a more detailed mineralogical analysis should be performed.

To summarize, the presented studies indicate the key factors that influence the distribution of ^{137}Cs activity concentrations in lake sediments of valley-type dam lake 32 years after the Chernobyl accident. The obtained results can be used to predict the long-term behavior of ^{137}Cs in the bottom sediments of reservoirs, which may be useful for radiological monitoring in other areas contaminated with cesium radioisotopes. This is particularly important, as it has been shown that dam lakes can accumulate large amounts of contaminated particles, which can pose a potential radiological hazard. The obtained results also showed that ^{137}Cs can be used as a tracer to reconstruct changes in sedimentation conditions over time in such lakes. It can be applicable, for example, in the case of studies concerning the problem of reservoir siltation. Moreover, considering climate change and the growing demand for electricity and drinking water, the presented conclusions may be relevant for the construction of a dam in areas contaminated with ^{137}Cs in the future.

Supplementary Information The online version contains supplementary material available at https://doi.org/10.1007/s11368-022-03326-5.

Acknowledgements The authors would like to thank the Editor and Reviewers for their careful reading of the manuscript and helpful comments. We also thank M. Syczewski from the Faculty of Geology of the University of Warsaw for his help in SEM–EDS analysis. The authors would also like to thank A. Huć from the Faculty of Geology of the University of Warsaw for her help in editing a graphic.

Author contribution I. Sekudewicz: conceptualization, methodology, sample collection, formal analysis, investigation, visualization, writing—original draft, writing—review and editing. Š. Matoušková: formal analysis. Z. Ciesielska: formal analysis. A. Mulczyk: formal analysis. M. Gąsiorowski: conceptualization, sample collection, supervision.

Funding This work was supported by the Institute of Geological Sciences of the Polish Academy of Sciences as an internal project for young scientists. Analyses with a laser particle size analyzer were funded by the institutional project RVO67985831 of the Institute of Geology of the Czech Academy of Sciences.

Declarations

Competing interests The authors declare no competing interests.

References

Appleby PG (2008) Three decades of dating recent sediments by fallout radionuclides: a review. Holocene 18(1):83–93. https://doi.org/10.1177/0959683607085598

Ashraf MA, Akib S, Maah MJ, Yusoff I, Balkhair KS (2014) Cesium-137: Radio-chemistry, fate, and transport, remediation, and future concerns. Crit Rev Environ Sci Technol 44:1740–1793. https://doi.org/10.1080/10643389.2013.790753

Belousov P, Semenkova A, Egorova T et al (2019) Cesium sorption and desorption on glauconite, bentonite, zeolite and diatomite. Minerals 9:625. https://doi.org/10.3390/min9100625

Beresford NA, Fesenko S, Konoplev A, Skuterud L, Smith JT, Voigt G (2016) Thirty years after the Chernobyl accident: what lessons have we learnt? J Environ Radioact 157:77–89. https://doi.org/10.1016/j.jenvrad.2016.02.003

Betancourt C, Jorge F, Suárez R, Beutel M, Gebremariam S (2010) Manganese sources and cycling in a tropical eutrophic water supply reservoir, Paso Bonito Reservoir. Cuba Lake Reserv Manag 26:217–226. https://doi.org/10.1080/07438141.2010.519856

Bobos I, Madruga MJ, Reis M, Esteves J, Guimarães V (2021) Clay mineralogy insights and assessment of the natural (^{228}Ra, ^{226}Ra, ^{210}Pb, ^{40}K) and anthropogenic (^{137}Cs) radionuclides dispersion in the estuarine and lagoon systems along the Atlantic coast of Portugal. Catena 206:105532. https://doi.org/10.1016/J.CATENA.2021.105532

Carlsson S (1978) A model for the movement and loss of ^{137}Cs in a small watershed. Health Phys 34:33–37. https://doi.org/10.1097/00004032-197801000-00002

Cieśla W, Malczyk P, Kędzia W, Majle T, Pachocki K (1994) ^{137}Cs i ^{134}Cs w glebach województwa bydgoskiego. Zesz Probl Postępów Nauk Rol 414:11–20

Contreras S, Werne JP, Araneda A, Urrutia R, Conejero CA (2018) Organic matter geochemical signatures (TOC, TN, C/N ratio, δ13C and δ15N) of surface sediment from lakes distributed along a climatological gradient on the western side of the southern Andes. Sci Total Environ 630:878–888. https://doi.org/10.1016/J.SCITOTENV.2018.02.225

Cornell RM (1993) Adsorption of cesium on minerals: a review. J Radioanal Nucl Chem Artic 171:483–500. https://doi.org/10.1007/BF02219872

Cremers A, Elsen A, De Preter P, Maes A (1988) Quantitative analysis of radiocaesium retention in soils. Nat 335:247–249. https://doi.org/10.1038/335247a0

De La Rocha CL, Nowald N, Passow U (2008) Interactions between diatom aggregates, minerals, particulate organic carbon, and dissolved organic matter: further implications for the ballast hypothesis. Global Biogeochem Cy 22(4). https://doi.org/10.1029/2007GB003156

Díaz-Asencio M, Corcho-Alvarado JA, Cartas-Aguila H et al (2017) ^{210}Pb and ^{137}Cs as tracers of recent sedimentary processes in two water reservoirs in Cuba. J Environ Radioact 177:290–304. https://doi.org/10.1016/J.JENVRAD.2017.07.005

Ertel JR, Hedges JI (1984) The lignin component of humic substances: distribution among soil and sedimentary humic, fulvic, and base-insoluble fractions. Geochim Cosmochim Ac 48:2065–2074. https://doi.org/10.1016/0016-7037(84)90387-9

Evans DW, Alberts JJ, Clark RA (1983) Reversible ion-exchange fixation of cesium-137 leading to mobilization from reservoir sediments. Geochim Cosmochim Ac 47:1041–1049. https://doi.org/10.1016/0016-7037(83)90234-X

Evrard O, Chaboche PA, Ramon R, Foucher A, Laceby JP (2020) A global review of sediment source fingerprinting research incorporating fallout radiocesium (^{137}Cs). Geomorphology 362:107103. https://doi.org/10.1016/J.GEOMORPH.2020.107103

Fan Q, Tanaka K, Sakaguchi A, Kondo H, Watanabe N, Takahashi Y (2014). Factors Controlling Radiocesium Distribution in River Sediments: Field and Laboratory Studies after the Fukushima Dai-Ichi Nuclear Power Plant Accident. https://doi.org/10.1016/j.apgeochem.2014.07.012

Foster IDL, Collins AL, Naden PS, Sear DA, Jones JI, Zhang Y (2011) The potential for paleolimnology to determine historic sediment delivery to rivers. J Paleolimnol 45:287–306. https://doi.org/10.1007/S10933-011-9498-9

Frink CR (1969) Chemical and mineralogical characteristics of eutrophic lake sediments. Soil Sci Soc Am J 33:369–372. https://doi.org/10.2136/SSSAJ1969.03615995003300030012X

Fujii M, Ono K, Yoshimura C, Miyamoto M (2018) The role of autochthonous organic matter in radioactive cesium accumulation to riverine fine sediments. Water Res 137:18–27. https://doi.org/10.1016/J.WATRES.2018.02.063

Funaki H, Yoshimura K, Sakuma K, Iri S, Oda Y (2019) Evaluation of particulate ^{137}Cs discharge from a mountainous forested catchment using reservoir sediments and sinking particles. J Environ Radioact 210:105814. https://doi.org/10.1016/J.JENVRAD.2018.09.012

Hagiwara H, Konishi H, Nakanishi T et al (2020) Mineral composition characteristics of radiocesium sorbed and transported sediments within the Tomioka river basin in Fukushima Prefecture. J Environ Radioact 211:106042. https://doi.org/10.1016/j.jenvrad.2019.106042

Hamilton NE, Ferry M (2018) ggtern: ternary diagrams using ggplot2. J Stat Softw Code Snippets 87(3):1–17. https://doi.org/10.18637/jss.v087.c03

Hazotte AA, Peron O, Abdelouas A, Montavon G, Lebeau T (2016) Microbial mobilization of cesium from illite: the role of organic acids and siderophores. Chem Geol 428:8–14. https://doi.org/10.1016/j.chemgeo.2016.02.024

He Q, Walling DE (1996) Interpreting particle size effects in the adsorption of ^{137}Cs and unsupported ^{210}Pb by mineral soils and sediments. J Environ Radioact 30:117–137. https://doi.org/10.1016/0265-931X(96)89275-7

Hilton J, Lishman JP, Allen PK (1986) The dominant processes of sediment distribution and focusing in a small, eutrophic, monomictic lake. Limnol Ocean 31:125–133

Huon S, Hayashi S, Laceby JP, Tsuji H, Onda Y, Evrard O (2018) Source dynamics of radiocesium-contaminated particulate matter deposited in an agricultural water reservoir after the Fukushima nuclear accident. Sci Total Environ 612:1079–1090. https://doi.org/10.1016/J.SCITOTENV.2017.07.205

Hydropower Plant Koronowo (2015) Data set of inflow (outflow) of water to (from) Koronowski Reservoir 1962–2015. Unpublished work

Ivanov MM, Konoplev AV, Walling DE et al (2021) Using reservoir sediment deposits to determine the longer-term fate of chernobyl-derived ^{137}Cs fallout in the fluvial system. Environ Pollut 274. https://doi.org/10.1016/J.ENVPOL.2021.116588

Kaminski S, Richter T, Walser M, Lindner G (1994) Redissolution of cesium radionuclides from sediments of freshwater lakes due to biological degradation of organic matter. Radiochimca Acta 66–67:433–436. https://doi.org/10.1524/ract.1994.6667.special-issue.433

Keil RG, Tsamakis E, Fuh CB, Giddings JC, Hedges JI (1994) Mineralogical and textural controls on the organic composition of coastal marine sediments: hydrodynamic separation using SPLITT-fractionation. Geochim Cosmochim Ac 58:879–893. https://doi.org/10.1016/0016-7037(94)90512-6

Kim Y, Cho S, Kang HD, Kim W et al (2006) Radiocesium reaction with illite and organic matter in marine sediment. Mar Pollut Bull 52:659–665. https://doi.org/10.1016/j.marpolbul.2005.10.017

Kim Y, Kim K, Kang HD et al (2007) The accumulation of radiocesium in coarse marine sediment: effects of mineralogy and organic matter. Mar Pollut Bull 54:1341–1350. https://doi.org/10.1016/J.MARPOLBUL.2007.06.003

Kim Y, Kirkpatrick RJ, Cygan RT (1996) ^{133}Cs NMR study of cesium on the surfaces of kaolinite and illite. Geochim Cosmochim Ac 60:4059–4074. https://doi.org/10.1016/S0016-7037(96)00257-8

Klaminder J, Appleby P, Crook P, Renberg I (2012) Post-deposition diffusion of ^{137}Cs in lake sediment: implications for radiocaesium dating. Sedimentology 59:2259–2267. https://doi.org/10.1111/j.1365-3091.2012.01343.x

Kobets SA, Fedorova VM, Pshinko GN et al (2014) Effect of humic acids and iron hydroxides deposited on the surface of clay minerals on the ^{137}Cs immobilization. Radiochemistry 56:325–331. https://doi.org/10.1134/S1066362214030175

Konoplev AV, Ivanov MM, Golosov VN, Konstantinov EA (2019) Reconstruction of long-term dynamics of Chernobyl-derived ^{137}Cs in the Upa River using bottom sediments in the Scheckino reservoir and semi-empirical modelling. Proc Int Assoc Hydrol Sci 381:95–99. https://doi.org/10.5194/piahs-381-95-2019

Konoplev A, Wakiyama Y, Wada T et al (2022) Reconstruction of time changes in radiocesium concentrations in the river of the Fukushima Dai-ichi NPP contaminated area based on its depth distribution in dam reservoir's bottom sediments. Environ Res 206:112307. https://doi.org/10.1016/J.ENVRES.2021.112307

Kónya J, Nagy NM, Nemes Z (2005) The effect of mineral composition on the sorption of cesium ions on geological formations. J Colloid Interface Sci 290:350–356. https://doi.org/10.1016/j.jcis.2005.04.082

Kurikami H, Kitamura A, Thomas Yokuda S, Onishi Y (2014) Sediment and ^{137}Cs behaviors in the Ogaki Dam Reservoir during a heavy rainfall event. J Environ Radioact 137:10–17. https://doi.org/10.1016/j.jenvrad.2014.06.013

Lamb AL, Wilson GP, Leng MJ (2006) A review of coastal palaeoclimate and relative sea-level reconstructions using δ13C and C/N ratios in organic material. Earth-Science Rev 75:29–57. https://doi.org/10.1016/J.EARSCIREV.2005.10.003

Livens FR, Baxter MS (1988) Particle size and radionuclide levels in some west Cumbrian soils. Sci Total Environ 70:1–17. https://doi.org/10.1016/0048-9697(88)90248-3

Luettich RA, Harleman DRF, Somlycidy L (1990) Dynamic behavior of suspended sediment concentrations in a shallow lake perturbed by episodic wind events. Limnol Ocean 35:1050–1067

Madruga MJ, Silva L, Gomes AR, Libânio A, Reis M (2014) The influence of particle size on radionuclide activity concentrations in Tejo River sediments. J Environ Radioact 132:65–72. https://doi.org/10.1016/J.JENVRAD.2014.01.019

Meyers PA, Ishiwatari R (1993) Lacustrine organic geochemistry-an overview of indicators of organic matter sources and diagenesis in lake sediments. Org Geochem 20:867–900. https://doi.org/10.1016/0146-6380(93)90100-P

Meyers PA, Ishiwatari R (1995) Organic matter accumulation records in lake sediments. Phys Chem Lakes 279–328. https://doi.org/10.1007/978-3-642-85132-2_10

Mouri G (2020) Reproduction of sediment deposition and prediction of ^{137}Cs concentration in the major urban rivers of Tokyo. Sci Rep 10:4–6. https://doi.org/10.1038/s41598-020-65700-y

Mukai H, Hirose A, Motai S et al (2016) Cesium adsorption/desorption behavior of clay minerals considering actual contamination conditions in Fukushima. Sci Rep 6:21543. https://doi.org/10.1038/srep21543

Muuri E, Ikonen J, Matara-aho M et al (2016) Behavior of Cs in Grimsel granodiorite. Sorption on main minerals and crushed rock. Radiochim Acta 104:575–582

Naulier M, Eyrolle-Boyer F, Boyer P et al (2017) Particulate organic matter in rivers of Fukushima: an unexpected carrier phase for radiocesiums. Sci Total Environ 579:1560–1571. https://doi.org/10.1016/j.scitotenv.2016.11.165

Nenadović S, Kljajević L, Marković S et al (2015) Natural diatomite (Rudovci, Serbia) as adsorbent for removal Cs from radioactive waste liquids. Sci Sinter 47:299–309. https://doi.org/10.2298/SOS1503299N

O'Connell DW, Mark Jensen M, Jakobsen R et al (2015) Vivianite formation and its role in phosphorus retention in Lake Ørn, Denmark. Chem Geol 409:42–53. https://doi.org/10.1016/J.CHEMGEO.2015.05.002

Park CW, Kim SM, Kim I et al (2021) Sorption behavior of cesium on silt and clay soil fractions. J Environ Radioact 233:106592. https://doi.org/10.1016/J.JENVRAD.2021.106592

Poinssot C, Baeyens B, Bradbury MH (1999) Experimental and modelling studies of caesium sorption on illite. Geochim Cosmochim Acta 63:3217–3227. https://doi.org/10.1016/S0016-7037(99)00246-X

Prahl FG, Bennett JT, Carpenter R (1980) The early diagenesis of aliphatic hydrocarbons and organic matter in sedimentary particulates from Dabob Bay, Washington. Geochim Cosmochim Ac 44:1967–1976. https://doi.org/10.1016/0016-7037(80)90196-9

Putyrskaya V, Klemt E (2007) Modelling ^{137}Cs migration processes in lake sediments. J Environ Radioact 96:54–62. https://doi.org/10.1016/j.jenvrad.2007.01.017

Putyrskaya V, Klemt E, Röllin S, Corcho-Alvarado JA, Sahli H (2020) Dating of recent sediments from Lago Maggiore and Lago di Lugano (Switzerland/Italy) using ^{137}Cs and ^{210}Pb. J Environ Radioact 212:106135. https://doi.org/10.1016/J.JENVRAD.2019.106135

Raven MD, Self PG (2017) Outcomes of 12 Years of the Reynolds Cup Quantitative Mineral Analysis Round Robin. Clays Clay Miner 65:122–134

R Core Team (2020) R: a language and environment for statistical computing. R Foundation for Statistical Computing, Vienna, Austria

Rigol A, Vidal M, Rauret G (2002) An overview of the effect of organic matter on soil-radiocaesium interaction: implications in root uptake. J Environ Radioact 58:191–216. https://doi.org/10.1016/S0265-931X(01)00066-2

Robbins JA, Krezoski JR, Mozley SC (1977) Radioactivity in sediments of the Great Lakes: post-depositional redistribution by deposit-feeding organisms. Earth Planet Sci Lett 36:325–333. https://doi.org/10.1016/0012-821X(77)90217-5

Sawhney BL (1972) Selective sorption and fixation of cations by clay minerals. A Rev Clays Clay Miner 20:93–100. https://doi.org/10.1346/CCMN.1972.0200208

Sedláček J, Bábek O, Grygar TM et al (2022) A closer look at sedimentation processes in two dam reservoirs. J Hydrol 605:127397. https://doi.org/10.1016/J.JHYDROL.2021.127397

Shepard FP (1954) Nomenclature based on sand-silt-clay ratios. J Sed Pet 24:151–158

Sekudewicz I, Gąsiorowski M (2022) Spatial and vertical distribution of ^{137}Cs activity concentrations in lake sediments of Turawa Lake (Poland). Environ Sci Pollut Res Int. https://doi.org/10.1007/s11356-022-21417-1

Somboon S, Kavasi N, Sahoo SK et al (2018) Radiocesium and ^{40}K distribution of river sediments and floodplain deposits in the Fukushima exclusion zone. J Environ Radioact 195:40–53. https://doi.org/10.1016/j.jenvrad.2018.09.003

Spezzano P (2005) Distribution of pre- and post-Chernobyl radiocaesium with particle size fractions of soils. J Environ Radioact 83:117–127. https://doi.org/10.1016/J.JENVRAD.2005.02.002

Środoń J, Drits VA, McCarty DK, Hsieh JC, Eberl DD (2001) Quantitative X-ray diffraction analysis of clay-bearing rocks from random preparations. Clays Clay Miner 49(6):514–528

Staunton S, Dumat C, Zsolnay A (2002) Possible role of organic matter in radiocaesium adsorption in soils. J Environ Radioact 58:163–173. https://doi.org/10.1016/S0265-931X(01)00064-9

Suga H, Fan Q, Takeichi Y et al (2014) Characterization of particulate matters in the Pripyat River in Chernobyl related to their adsorption of radiocesium with inhibition effect by natural organic matter. Chem Lett 43(7):1128–1130. https://doi.org/10.1246/CL.140222

Szatten D (2016) Proposal of a new hydromporphometric division of Koronowski reservoir (in Polish). Geograph Tour 4:79–84. https://doi.org/10.5281/zenodo.56746

Szatten D, Habel M, Pellegrini L, Maerker M (2018) Assessment of siltation processes of the Koronowski Reservoir in the northern Polish lowland based on bathymetry and empirical formulas. Water 10(11):1681. https://doi.org/10.3390/w10111681

Tachi Y, Sato T, Akagi Y et al (2020a) Key factors controlling radiocesium sorption and fixation in river sediments around the Fukushima Daiichi Nuclear Power Plant. Part 1: insights from sediment properties and radiocesium distributions. Sci Total Environ 724:138098. https://doi.org/10.1016/J.SCITOTENV.2020.138098

Tachi Y, Sato T, Takeda C et al (2020b) Key factors controlling radiocesium sorption and fixation in river sediments around the Fukushima Daiichi Nuclear Power Plant. Part 2: Sorption and fixation behaviors and their relationship to sediment properties. Sci Total Environ 724:138097. https://doi.org/10.1016/J.SCITOTENV.2020.138097

Tadejewski A (1966) Bottom sediments in different limnetic zones of an eutrophic lake. Ekol Pol A 14:1–21

Tamura T, Jacobs DG (1960) Structural implications in cesium sorption. Health Phys 2:391–398. https://doi.org/10.1097/00004032-195910000-00009

Tanaka K, Iwatani H, Sakaguchi A, Fan Q, Takahashi Y (2015) Size-dependent distribution of radiocesium in riverbed sediments and its relevance to the migration of radiocesium in river systems after the Fukushima Daiichi Nuclear Power Plant accident. J Environ Radioact 139:390–397. https://doi.org/10.1016/J.JENVRAD.2014.05.002

Tsuji H, Tanaka A, Komatsu K et al (2019) Vertical/spatial movement and accumulation of ^{137}Cs in a shallow lake in the initial phase after the Fukushima Daiichi nuclear power plant accident. Appl Radiat Isot 147:59–69. https://doi.org/10.1016/J.APRADISO.2019.02.009

Waters MN, Golladay SW, Patrick CH, Smoak JM, Shivers SD (2015) The potential effects of river regulation and watershed land use on sediment characteristics and lake primary producers in a large reservoir. Hydrobiologia 749:15–30. https://doi.org/10.1007/S10750-014-2142-8

Wieczorek D, Stoiński A (2008) Detailed geological map of Poland in scale 1:50 000. Map series: 241 – Gostycyn (N-33-96-D). Polish Geological Institute (PGI). https://bazadata.pgi.gov.pl/data/smgp/arkusze_skany/smgp0241.jpg

Wilkin RT, Barnes HL, Brantley SL (1996) The size distribution of framboidal pyrite in modern sediments: an indicator of redox conditions. Geochim Cosmochim Ac 60:3897–3912. https://doi.org/10.1016/0016-7037(96)00209-8

Zachara JM, Smith S, Liu C et al (2002) Sorption of Cs^+ to micaceous subsurface sediments from the Hanford Site, USA. Geochim Cosmochim Acta 66:193–211. https://doi.org/10.1016/S0016-7037(01)00759-1

Zapata F, Nguyen ML (2009) Soil erosion and sedimentation studies using environmental radionuclides, in: Froehlich, K., (Eds.), Environmental radionuclides: tracers and timers of terrestrial processes. Radioactivity in the Environment. Elsevier 16:295–322. https://doi.org/10.1016/S1569-4860(09)01607-6